Comprehensive Resonance Raman Study of Photosynthetic Reaction Centers from *Rhodobacter sphaeroides*. Implications for Pigment Structure and Pigment–Protein Interactions

Vaithianathan Palaniappan,† Paul C. Martin,† Veeradej Chynwat,‡ Harry A. Frank,‡ and David F. Bocian*,†

Contribution from the Departments of Chemistry, University of California, Riverside, California 92521, and University of Connecticut, Storrs, Connecticut 06269

Received July 14, 1993®

Abstract: Resonance Raman (RR) spectra are reported for photosynthetic reaction centers (RC's) from the purple bacterium *Rhodobacter sphaeroides*. The spectra of quinone-reduced RC's were obtained by using a large number of excitation wavelengths (23) in the 335–875-nm range. These wavelengths span the B_x, B_y, Q_x, and Q_y absorption bands of the special pair bacteriochlorophyll (P), accessory bacteriochlorophyll (BCh), and bacteriopheophytin (BPh) pigments. The number of exciting lines and their wavelengths were chosen to optimize the selective excitation of the different pigments in the RC and to elicit the full complement of RR scattering from the individual pigments. The RR spectra of the quinone-reduced RC's were compared with one another and with those of chemically oxidized RC's, tetrapyrrolic model compounds, and BCh/BPh in solution. On the basis of these comparisons, a self-consistent set of vibrational assignments is proposed for the high-frequency (1425–1750 cm^{-1}) carbonyl and skeletal modes of the six bacteriochlorin pigments in the protein. These assignments were aided by the results of semiempirical normal coordinate calculations. Collectively, the vibrational data and assignments indicate the following: (1) A reasonable set of vibrational assignments can be obtained. These assignments show that previous assignments for certain high-frequency modes and the interpretation of oxidation-induced frequency shifts observed in both static and time-resolved vibrational spectra must be reconsidered. (2) The structures of the L- and M-side accessory BCh's are essentially identical and similar to those of 5-coordinate BCh in solution. (3) The structures of the BCh's in P do not appear to be identical. The structure of one pigment of P is similar to that of the accessory BCh's. The vibrational frequencies of the other are consistent with either an expanded macrocycle core or a more conformationally distorted ring. (4) The structures of the L- and M-side BPh's are for the most part alike and similar to those of BPh in solution. However, the structure of BPh_L in the region of rings III and V is different from that of BPh_M. This difference is due to the interaction of the C_9-keto group of BPh_L with the Glu_{L104} residue. An equivalent pigment–protein interaction is absent on the M-side.

I. Introduction

The primary electron-transfer processes in bacterial photosynthesis occur in a specialized unit of membrane-bound pigments known as the reaction centers (RC's).[1-5] Bacterial RC's consist of four bacteriochlorophylls (BCh's), two bacteriopheophytins (BPh's), two quinones, a non-heme iron center, a carotenoid (CAR), and ~850 amino acid residues in three polypeptide subunits designated by L, M, and H. The primary donor in the electron-transfer process is a closely associated pair of BCh's, known as the special pair (P). The primary acceptor is the BPh pigment in the L-subunit.[2,5-7] The X-ray crystal structures of RC's from two different purple bacteria (*Rhodobacter sphaeroides* and *Rhodopseudomonas viridis*) have been determined.[8-10] These structures reveal that the BCh and BPh pigments are arranged in the L- and M-subunits such that the macroscopic symmetry is approximately C_2. However, this symmetry is broken by subunit-specific pigment–protein interactions. There are also asymmetries in L- versus M-side amino acid residues which do not directly interact with the pigments. A schematic representation of the RC showing the various cofactors (excluding the CAR) is presented in Figure 1. The specific pigment–protein interactions proposed by the Argonne group, based on their crystal structure of RC's from *Rb. sphaeroides*, are indicated in the figure.[10c] The asymmetrical distribution of amino acid residues in the L- versus M-subunits is presumably responsible for the fact that the primary electron-transfer proceeds along the L-side.[11] The possibility that certain protein residues might be responsible for the path specificity of electron transfer has led to the characterization of a variety of genetically modified RC's in which the L- versus M-side asymmetries have been altered.[12-15] To date, however, no mutations have been made that alter the path specificity of electron transfer.

Two types of pigment–protein interactions are illustrated in Figure 1. The first is hydrogen bonding between a protein residue and one of the four different carbonyi groups of the BCh and BPh

† University of California.
‡ University of Connecticut.
® Abstract published in *Advance ACS Abstracts*, November 15, 1993.

(1) Budil, D.; Gast, P.; Schiffer, M.; Norris, J. R. *Annu. Rev. Phys. Chem.* **1987**, *38*, 561–583.
(2) Kirmaier, C.; Holten, D. *Photosynth. Res.* **1987**, *113*, 225–260.
(3) Deisenhofer, J.; Michel, H. *Science* **1989**, *245*, 1463–1473.
(4) (a) Feher, G. *Annu. Rev. Phys. Chem.* **1989**, *58*, 607–663. (b) Feher, G.; Allen, J. P.; Okamura, M. Y.; Rees, D. C. *Nature* **1989**, *339*, 111–116.
(5) Boxer, S. G.; Goldstein, R. A.; Lockhart, D. J.; Middendorf, R. T.; Takiff, L. *J. Phys. Chem.* **1989**, *93*, 8280–8294.
(6) Friesner, R. A.; Won, Y. *Biochim. Biophys. Acta* **1989**, *977*, 99–122.
(7) For a recent monograph, see: Breton, J; Verméglio, A., Eds. *NATO ASI Ser., Ser. A* **1992**, *237*, 1–429.
(8) (a) Deisenhofer, J.; Epp, O.; Miki, R.; Huber, R.; Michel, H. *Nature* **1985**, *339*, 618–624. (b) Deisenhofer, J.; Michel, H. *EMBO J.* **1989**, *8*, 2149–2169. (c) Deisenhofer, J.; Michel, H. *Annu. Rev. Cell Biol.* **1991**, *7*, 1–23. (d) Deisenhofer, J.; Michel, H. *Annu. Rev. Biophys. Biophys. Chem.* **1991**, *20*, 247–266.
(9) (a) Allen, J. P.; Feher, G.; Yeates, T. O.; Rees, D. C.; Deisenhofer, J.; Michel, H.; Huber, R. *Proc. Natl. Acad. Sci. U.S.A.* **1986**, *83*, 8589–8593. (b) Allen, J. P.; Feher, G.; Yeates, T. O.; Komiya, H.; Rees, D. C. *Proc. Natl. Acad. Sci. U.S.A.* **1988**, *85*, 8487–8491. (c) Yeates, T. O.; Komiya, H.; Chirino, A.; Rees, D. C.; Allen, J. P.; Feher, G. *Proc. Natl. Acad. Sci. U.S.A.* **1988**, *85*, 7993–7997.
(10) (a) Chang, C.-H.; Tiede, D.; Tang, J.; Smith, U.; Norris, J.; Schiffer, M. *FEBS Lett.* **1986**, *205*, 82–86. (b) Chang, C.-H.; El-Kabbani, O.; Tiede, D.; Norris, J.; Schiffer, M. *Biochemistry* **1991**, *30*, 5352–5360. (c) El-Kabbani, O.; Chang, C.-H.; Tiede, D.; Norris, J.; Schiffer, M. *Biochemistry* **1991**, *30*, 5361–5369.
(11) Kirmaier, C.; Holten, D.; Parson, W. W. *Biochim. Biophys. Acta* **1985**, *810*, 49–61.

0002-7863/93/1515-12035$04.00/0

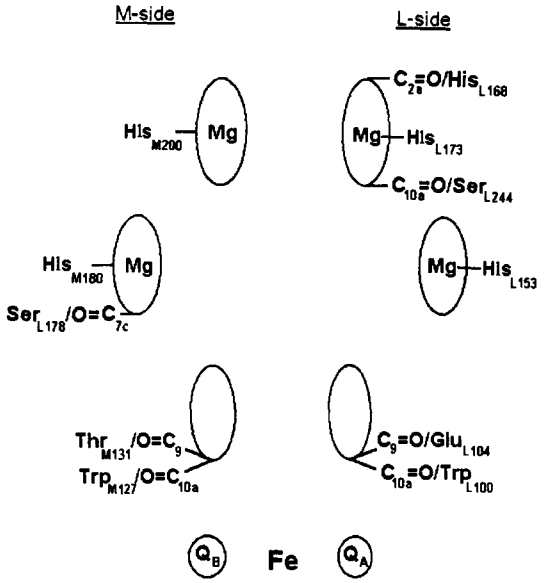

Figure 1. Schematic representation of the RC from *Rb. sphaeroides* showing the organization of various cofactors (BCh, BPh, the quinones (Q_A and Q_B), and the nonheme iron center). The CAR (spheroidene) is not shown. The protein residues which are in sufficiently close proximity to interact with the BCh's and BPh's are also indicated in the figure. The interactions shown are those proposed by the Argonne group on the basis of the X-ray crystal structure of RC's from the carotenoidless mutant *Rb. sphaeroides* R-26 (ref 10c) and include hydrogen bonding to the various carbonyl groups and axial ligation of the Mg(II) ions of the BCh's.

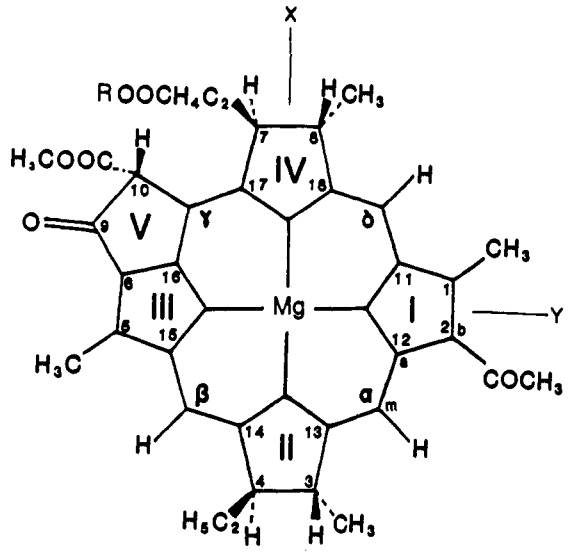

Figure 2. Schematic representation of the structure and labeling scheme for BCh.

pigments. The locations of these carbonyl groups on the bacteriochlorin ring are shown in Figure 2. Of the four different carbonyls, two (C_9-keto and C_2-acetyl) are conjugated with the π system of the bacteriochlorin macrocycle and two (C_{10}-carbomethoxy and C_7-propionic acid) are not. Hydrogen-bonding interactions with the carbonyl groups, particularly the conjugated C_9-keto and C_2-acetyl groups, are expected to alter the redox potential of the macrocycle via direct electronic effects.[14h] The redox potential could also be affected if the hydrogen-bonding interaction influences the conformation of the bacteriochlorin macrocycle. In this regard, highly nonplanar porphyrins are known to exhibit much lower oxidation potentials than more planar forms.[16] The second type of pigment–protein interaction shown in Figure 1 is the axial ligation of the Mg(II) ions of the accessory BCh's and the BCh's in P by histidine residues in the L- and M-subunits. The strength of this interaction is expected to determine the position of the metal ion with respect to the plane of the bacteriochlorin macrocycle. The position of the metal ion would affect the conformation of the ring and potentially its redox chemistry. The crystallographically determined structures of RC's from both *Rps. viridis* and *Rb. sphaeroides* indicate that there are indeed differences in the Mg–histidine bond lengths in P_L versus P_M and BCh_L versus BCh_M.[8b,9c,10c] However, in the case of *Rb. sphaeroides*, there is controversy concerning the magnitude of the L- versus M-side Mg(II)–histidine bond length disparities.[9c,10c]

Vibrational spectroscopy offers an excellent opportunity to probe the structures of the pigments in RC's and to examine the effects of pigment–protein interactions. Both resonance Raman (RR) and Fourier-transform infrared (FT-IR) techniques have been used to study RC's.[13,15,17] Most of these studies have focused on the carbonyl groups of the BCh and BPh pigments of RC's and the nature of the hydrogen-bonding interactions between these groups and the protein. On the basis of a series of RR studies, Lutz and co-workers have proposed assignments for the C_9-keto and C_2-acetyl carbonyl stretches of all six bacteriochlorin pigments in the RC.[17c,18] These workers have also examined the RR spectra of RC's in which P is chemically or photochemically oxidized and explored the carbonyl frequency shifts associated with the formation of P^+.[18,19] Breton, Mäntele, and others have examined the FT-IR spectra of RC's under a variety of

(12) (a) Bylina, E. J.; Youvan, D. C. *Z. Naturforsch.* **1987**, *42C*, 769–774. (b) Bylina, E. J.; Youvan, D. C. *Proc. Natl. Acad. Sci. U.S.A.* **1988**, *85*, 7226–7230. (c) Bylina, E. J.; Kirmaier, C.; McDowell, L.; Holten, D.; Youvan, D. C. *Nature* **1988**, *336*, 182–184. (c) Bylina, E. J.; Robles, S.; Youvan, D. C. *Isr. J. Chem.* **1988**, *28*, 73–78. (d) Breton, J.; Bylina, E. J.; Youvan, D. C. *Biochemistry* **1989**, *28*, 6423–6430. (e) Kirmaier, C.; Bylina, E. J.; Youvan, D. C.; Holten, D. *Chem. Phys. Lett.* **1989**, *159*, 251–257. (f) Bylina, E. J.; Kowlaczkowski, S. V.; Norris, J. R.; Youvan, D. C. *Biochemistry* **1990**, *29*, 6203–6210. (g) Coleman, W. J.; Youvan, D. C. *Annu. Rev. Biophys. Biophys. Chem.* **1990**, *19*, 333–367. (h) DiMagno, T. J.; Bylina, E. J.; Angerhofer, A.; Youvan, D. C.; Norris, J. R. *Biochemistry* **1990**, *29*, 899–907 (i) McDowell, L. M.; Kirmaier, C.; Holten, D. *J. Phys. Chem.* **1991**, *95*, 3379–3383. (j) Chan, C.-K.; Chen. L. X.-Q.; DiMagno, T. J.; Hanson, D. K.; Nance, S. L.; Schiffer, M.; Norris, J. R.; Fleming, G. *Chem. Phys. Lett.* **1991**, *176*, 182–184. (k) Du, M.; Rosenthal, S. J.; Xie, X.; DiMagno, T. J.; Schmidt, M.; Hanson, D. K.; Schiffer, M.; Norris, J. R.; Fleming, G. R. *Proc. Natl. Acad. Sci. U.S.A.* **1992**, *89*, 8517–8521. (l) Taguchi, A. K. W.; Stocker, J. W.; Alden, R. G.; Causgrove, T. P.; Peloquin, J. M.; Boxer, S. G.; Woodbury, N. W. *Biochemistry* **1992**, *31*, 10345–10355. (m) Stocker, J. W.; Taguchi, A. K. W.; Murchison, H. A.; Woodbury, N. W.; Boxer, S. G. *Biochemistry* **1992**, *31*, 10356–10362. (n) Taguchi, A. K. W.; Stocker, J. W.; Boxer, S. G.; Woodbury, N. W. *Photosynth. Res.* **1993**, *36*, 43–58.

(13) (a) Peloquin, J. M.; Bylina, E. J.; Youvan, D. C.; Bocian, D. F. *Biochemistry* **1990**, *29*, 8417–8424. (b) Peloquin, J. M.; Bylina, E. J.; Youvan, D. C.; Bocian, D. F. *Biochim. Biophys. Acta* **1991**, *1056*, 85–88. (c) Nabedryk, E.; Robles, S. J.; Goldman, E.; Youvan, D. C.; Breton, J. *Biochemistry* **1992**, *31*, 10852–10858.

(14) (a) Farchaus, J. W.; Oesterhelt, D. *EMBO J.* **1989**, *8*, 47–54. (b) Finkele, U.; Lauterwasser, C.; Zinth, W.; Gray, K. A.; Oesterhelt, D. *Biochemistry* **1990**, *29*, 8517–8521. (c) Nagarajan, V.; Parson, W. W.; Gaul, D.; Schenck, C. *Proc. Natl. Acad. Sci. U.S.A.* **1990**, *87*, 7888–7892. (d) Hammes, S. L.; Mazzoli, L. T.; Boxer, S. G.; Gaul, D.; Schenck, C. C. *Proc. Natl. Acad. Sci. U.S.A.* **1990**, *87*, 5682–5686. (e) Middendorf, T. R.; Mazzoli, L. T.; Gaul, D. F.; Schenck, C. C.; Boxer, S. G. *J. Phys. Chem.* **1991**, *95*, 10142–10151. (f) Kirmaier, C.; Holten, D. *Biochemistry* **1991**, *30*, 609–613. (g) Kirmaier, C.; Gaul, D.; DeBey, R.; Holten, D.; Schenck, C. C. *Science* **1991**, *251*, 922–927. (h) Williams, J. C.; Alden, R. G.; Murchison, H. A.; Peloquin, J. M.; Woodbury, N. W.; Allen, J. P. *Biochemistry* **1992**, *31*, 11029–11037. (i) Murchison, H. A.; Alden, R. G.; Allen, J. P.; Peloquin, J. M.; Taguchi, A. K. W.; Woodbury, N. W.; Williams, J. C. *Biochemistry* **1993**, *32*, 3498–3505.

(15) (a) Mattioli, T. A.; Gray, K. A.; Lutz, M.; Oesterhelt, D.; Robert, B. *Biochemistry* **1991**, *30*, 1715–1722. (b) Nabedryk, E.; Breton, J.; Allen, J.; Murchison, H.; Taguchi, A.; Williams, J.; Woodbury, N. In ref 7, pp 141–145. (c) Nabedryk, E.; Breton, J.; Wachtveitl, J.; Gray, K. A.; Oesterhelt, D. In ref 7, pp 147–153.

(16) Barkigia, K. M.; Chantranupong, L.; Smith, K. M.; Fajer, J. *J. Am. Chem. Soc.* **1988**, *110*, 7566–7567.

(17) For reviews, see: (a) Lutz, M. *Adv. Infrared and Raman Spectrosc.* **1984**, *11*, 211–300. (b) Lutz, M.; Robert, B. In *Biological Applications of Raman Spectroscopy*; Spiro, T. G., Ed.; Wiley: New York, 1988; Vol. 3, pp 347–411. (c) Robert, B. *Biochim. Biophys. Acta* **1990**, *1017*, 99–111. (d) Lutz, M.; Mäntele, W. In *Chlorophylls*; Scheer, H., Ed.; CRC Press: Boca Raton, FL, 1991; pp 855–902.

(18) Robert, B.; Lutz, M. *Biochemistry* **1988**, *27*, 5108–5114.

(19) (a) Mattioli, T. A.; Hoffman, A.; Robert, B. Schrader, B.; Lutz, M. *Biochemistry* **1991**, *30*, 4648–4654. (b) Mattioli, T. A.; Robert, B.; Lutz, M. In ref 7, pp 127–132.

conditions.[13c,15b,c,17d,20-22] These workers have also primarily focused their attention on the carbonyl stretching vibrations of the pigments and the frequency shifts observed for these modes upon the formation of P^+.

Although potentially useful structural information has been extracted via examination of the carbonyl stretching vibrations of the BCh and BPh pigments in RC's, these modes alone cannot give a comprehensive picture of the structural consequences of incorporating the pigments into the protein matrix or the structural changes associated with the formation of P^+. In particular, the carbonyl stretches are not sensitive to the conformation of the macrocycle or to Mg(II)–axial ligand interactions. The modes most sensitive to these structural features are the skeletal vibrations of the macrocycle.[23-25] The structural sensitivity of the ring-skeletal modes of tetrapyrrolic macrocycles has been extensively exploited in RR studies of heme proteins.[26] In contrast, the skeletal modes have been the focal point of only a few RR studies of RC's. For this reason, we initiated RR studies aimed at characterizing the ring-skeletal vibrations of the BCh and BPh pigments in both wild-type and genetically modified RC's.[13a,b,27] Our previous work focused primarily on selected vibrations in the 1580–1615-cm^{-1} regime. However, the interpretation of these data was precluded by the absence of detailed vibrational assignments for the ring-skeletal modes of the pigments. Toward this goal, we undertook a comprehensive examination of the high-frequency (1425–1750 cm^{-1}) region of the RR spectra of RC's. The results are reported herein.

The RR spectra of quinone-reduced RC's from the purple bacterium *Rb. sphaeroides* 2.4.1 were obtained by using a large number of excitation wavelengths (23) in the 335–875-nm range. These wavelengths span the B_x, B_y, Q_x, and Q_y absorption bands of P, the accessory BCh's, and the BPh's. All previous RR studies of RC's have utilized only one or two exciting lines, principally in the B or Q_x absorptions[17] (although recently several Q_y-state-excitation RR studies have been reported[19,28-31]). The limited number of exciting lines used in earlier studies did not allow either the selective excitation of the different pigments in the RC or the observation of the full complement of RR bands from the individual pigments. In our studies, the number of exciting lines and their wavelengths were chosen to optimize both of these spectral characteristics. The RR spectra of the quinone-reduced RC's were compared with one another and with those of chemically oxidized RC's, tetrapyrrolic model compounds, and BCh/BPh in solution. On the basis of these comparisons and the predictions of semiempirical normal coordinate calculations, a self-consistent set of vibrational assignments in the 1425–1750-cm^{-1} region has been obtained for the six bacteriochlorin pigments in the protein. Collectively, the vibrational data and assignments provide new insights into the structures of the pigments and the nature of the pigment–protein interactions. The assignments also serve as benchmarks for interpreting static[17] and time-resolved[20e,f,32] vibrational spectra of RC's and for interpreting the spectra of genetically modified proteins.[13,15]

The organization of the paper is as follows. First, we present the results of the RR study and summarize the vibrational assignments for the BCh and BPh pigments in the RC. Next, we describe the general features of the RR spectra. We then discuss our general approach to obtaining a self consistent set of vibrational assignments and the assignments for individual modes of the different pigments. Finally, we comment on the structural implications of the vibrational assignments for the different pigments in the RC.

II. Materials and Methods

A. Sample Preparation. The RC's from *Rb. sphaeroides* 2.4.1 and the carotenoidless mutant R-26 were prepared as previously described.[33] The proteins were eluted from a DEAE anion-exchange column by using 0.01 M Tris (pH 8.0), 0.015% Triton X-100, and 0.5 M sodium chloride. The RC's were chemically reduced or oxidized by adding a slight excess of $Na_2S_2O_4$ or $K_3Fe(CN)_6$, respectively.

B. RR Spectroscopy. The RR measurements were made on glassed samples (~1:1 in ethylene glycol, total concentration ~35 μM) at 200 K contained in 1 mm i.d. capillary tubes. Temperature control was achieved by mounting the sample on the cold tip of a closed cycle refrigeration system (ADP Cryogenics, DE-202 Displex). The sample was excited transversely by placing a mirror directly above the capillary. The scattering was collected in a 90° configuration by using a camera lens (50 mm f/1.4 Canon FD lens for UV and violet and 50 mm f/1.4 Nikkor AF lens for red, near-infrared, and other colors) and dispersed by a 0.6 m triple spectrograph (Spex Industries 1877). Two different triple spectrographs were used for data acquisition. For excitation in the 335–550-nm region, the filter stage was equipped with 600 groove/mm gratings and the spectrograph stage was equipped with either 1800 or 2400 groove/mm gratings. All gratings were blazed at 550 nm. For excitation in the 600–875-nm region, the filter stage was equipped with 600 groove/mm gratings blazed at 750 nm. The spectrograph stage was equipped with either 600 or 1200 groove/mm gratings blazed at either 750 or 1000 nm. A polarization scrambler (Spex Industries) was placed in front of the entrance slit of the spectrometer. The detection system used for the UV- and violet-excitation experiments was an optical multichannel analyzer equipped with a UV and IR enhanced 1024 pixel intensified diode array head (EG&G Princeton Applied Research Corporation Models 1460 and 1421). The detection system used for the longer wavelength visible- and near-infrared-excitation experiments was a liquid nitrogen cooled (−120 °C) 512 × 512 pixel back-illuminated charge-coupled device (CCD) (Princeton Instruments LN/CCD with a Tektronix chip). The quantum efficiency of this CCD is ~50% at 850 nm and ~20% at 1000 nm. The high quantum efficiency of the back-illuminated CCD greatly facilitates the acquisition of good-quality high-

(20) (a) Mäntele, W.; Nabedryk, E.; Tavitian, B. A.; Kreutz, W.; Breton, J. *FEBS Lett.* **1985**, *187*, 227–232. (b) Nabedryk, E.; Mäntele, W.; Tavitian, B. A.; Breton, J. *Photochem. Photobiol.* **1986**, *43*, 461–465. (c) Mäntele, W.; Wollenweber, A.; Nabedryk, E.; Breton, J. *Proc. Natl. Acad. Sci. U.S.A.* **1988**, *85*, 8468–8472. (d) Nabedryk, E.; Bagley, K. A.; Thibodeau, D. L.; Bauscher, M.; Mäntele, W.; Breton, J. *FEBS Lett.* **1990**, *266*, 59–62. (e) Thibodeau, D. L.; Breton, J.; Berthomieu, C.; Bagley, K. A.; Mäntele, W.; Nabedryk, E. In *Reaction Centers of Photosynthetic Bacteria*; Michel-Beyerle, M.-E., Ed.; Springer: Berlin, 1990; Vol. 6, pp 87–98. (f) Heinerwadel, R.; Thibodeau, B.; Lenz, F.; Nabedryk, E.; Breton, J.; Kreutz, W.; Mäntele, W. *Biochemistry* **1992**, *31*, 5799–5808. (g) Breton, J.; Burie, J.-R.; Berthomieu, C.; Thibodeau, D. L.; Andranambinintsoa, S.; Dejonghe, D.; Berger, G.; Nabedryk, E. In ref 7, pp 155–162. (h) Heinerwadel, R.; Nabedryk, E.; Breton, J.; Kreutz, W.; Mäntele, W. In ref 7, pp 161–172. (i) Leonhard, M.; Mäntele, W. *Biochemistry* **1993**, *32*, 4532–4538.

(21) (a) Morita, E. H.; Hayashi, H.; Tasumi, M. *Chem. Lett.* **1991**, 1583–1586. (b) Morita, E. H.; Hayashi, H.; Tasumi, M. *Chem. Lett.* **1991**, 1853–1856. (c) Morita, E. H.; Hayashi, H.; Tasumi, M. *Biochim. Biophys. Acta* **1993**, *1142*, 146–154.

(22) (a) Gerwert, K.; Hess, B.; Michel, H.; Buchanan, S. *FEBS Lett.* **1988**, *232*, 303–307. (b) Buchanan, S.; Michel, H.; Gerwert, K. *Biochemistry* **1992**, *31*, 1314–1322.

(23) (a) Fujiwara, M.; Tasumi, M. *J. Phys. Chem.* **1986**, *90*, 250–255. (b) Fujiwara, M.; Tasumi, M. *J. Phys. Chem.* **1986**, *90*, 5646–5650. (c) Tasumi, M.; Fujiwara, M. *Adv. Spectrosc.* **1987**, *14*, 407–428.

(24) Callahan, P. M.; Cotton, T. M. *J. Am. Chem. Soc.* **1987**, *109*, 7001–7007.

(25) Schick, G. A.; Bocian, D. F. *Biochim. Biophys. Acta* **1987**, *895*, 127–154.

(26) For recent reviews, see: (a) Spiro, T. G., Ed. *Biological Applications of Raman Spectroscopy*; Wiley: New York, 1988; Vol. 3, pp 39–346. (b) Spiro, T. G.; Smulevich, G.; Su, C. *Biochemistry* **1990**, *29*, 4497–4508. (c) Palaniappan, V.; Sullivan, A. M.; Fitzgerald, M. M.; Shifflett, J. R.; Terner, J. In *Charge and Field Effects in Biosystems-3*; Allen, M. J., Cleary, S. F., Sowers, A. E., Shillady, D. D., Eds.; Birkhäuser: Boston, 1992; pp 349–364.

(27) Peloquin, J. M.; Violette, C. A.; Frank, H. A.; Bocian, D. F. *Biochemistry* **1990**, *29*, 4892–4898.

(28) (a) Bocian, D. F.; Boldt, N. J.; Chadwick, B. W.; Frank, H. A. *FEBS Lett.* **1987**, *214*, 92–96. (b) Donohoe, R. J.; Dyer, R. B.; Swanson, B. I.; Violette, C. A.; Frank, H. A.; Bocian, D. F. *J. Am. Chem. Soc.* **1990**, *112*, 6716–6718. (c) Palaniappan, V.; Bocian, D. F. In ref 7, pp 119–126. (d) Palaniappan, V.; Aldema, M. A.; Frank, H. A.; Bocian, D. F. *Biochemistry* **1992**, *31*, 11050–11058.

(29) (a) Johnson, C. K.; Rubinovitz, R. *Appl. Spectrosc.* **1990**, *44*, 1103–1106. (b) Johnson, C. K.; Rubinovitz, R. *Spectrochim. Acta* **1991**, *47A*, 1413–1421.

(30) Noguchi, T.; Furukawa, Y.; Tasumi, M. *Spectrochim. Acta* **1991**, *47A*, 1431–1440.

(31) Shreve, A. P.; Cherepy, N. J.; Franzen, S.; Boxer, S. G.; Mathies, R. A. *Proc. Natl. Acad. Sci. U.S.A.* **1991**, *88*, 11207–11211.

(32) Maiti, S.; Cowen, B. R.; Diller, R.; Iannone, M.; Moser, C. C.; Dutton, P. L.; Hochstrasser, R. M. *Proc. Natl. Acad. Sci. U.S.A.* **1993**, *90*, 5247–5251.

(33) McGann, W. J.; Frank, H. A. *Biochim. Biophys. Acta* **1985**, *807*, 101–109.

frequency RR spectra of P with near-infrared excitation. The excitation wavelengths were provided by the outputs of an Ar ion laser (Coherent Innova 400-15UV), a Kr ion laser (Coherent Innova 200-K3), a Ti:sapphire laser (Coherent 890), or a continuous wave dye laser (Coherent 599, utilizing the tuning range of Rhodamine 6G). The Ti:sapphire and dye lasers were pumped by the visible multiline output of the Ar ion laser. The laser powers at the sample were 0.3–1 mW for excitation in the red and near-infrared and 2–5 mW for all other experiments. The power density was lowered by defocusing the incident beam to illuminate a volume of 1–2 μL. The resulting photon fluxes (50–300 photons s^{-1} RC^{-1}) were low enough that less than 3% of the RC's existed in photogenerated transient states (P^+ or ^3P) at any of the excitation wavelengths used. In order to enhance the longevity of the samples, the capillary tubes were repositioned in the laser beam after every scan. Even small amounts of photodamage are discernible in the RR experiments because loss of sample integrity leads to highly fluorescent impurities. A standard data acquisition protocol consisted of the coaddition of four to eight 1-h (30 × 120 s) scans. Cosmic spikes in the individual data sets obtained with the CCD detector were removed prior to coaddition of the data sets. Typical slit widths used in the RR experiments yielded a spectral resolution of 1–4 cm^{-1} depending on the excitation wavelength and/or the spectral region in the data acquisition window.

The RR signals observed for the RC's were superimposed on a fluorescent background. The fluorescence is particularly intense in the red and near-infrared regions. In these regions, the intensities of the RR signals are in the 1–3% range of the total signal intensity. This level of RR signal intensity allows background removal via subtraction of a standard polynomial fit to the broad-band emission.[28c,d] Prior to background subtraction, the RR spectra were flat-field corrected by using a spectrally broad emission lamp. This type of background correction does not alter the frequencies of the RR bands but it does influence the relative intensities. Consequently, the relative intensities of the RR bands shown in the spectra acquired with red and near-infrared excitation are accurate to ±50%. We have discussed this issue in detail elsewhere.[28d]

Although good-quality RR spectra were obtained via background subtraction/flat-field correction, data were also obtained by using the shifted excitation-wavelength difference method in order to determine whether the background corrections introduced any spectral artifacts.[34] The application of this method to RC's has been previously described.[28d,31] Briefly, data sets were acquired at two excitation wavelengths which differ by small wavenumber increments (10–20 cm^{-1}). These data sets were then subtracted (without polynomial background subtraction/flat-field correction) to yield a background-corrected difference RR spectrum. Comparison of the spectra obtained in this fashion with those obtained in a standard RR experiment revealed that the polynomial background subtraction/flat-field correction did not introduce any artifacts in the spectra. The vibrational frequencies obtained by both techniques were calibrated by using the known frequencies of indene.

C. Normal Coordinate Calculations. The calculated vibrational frequencies and normal coordinates for the high-frequency modes of BCh were obtained by using the QCFF/PI method.[35] The calculations were performed as previously described in our analysis of Cu(II) bacteriopheophytin *a*.[36] In the present calculations, the Cu(II) atom was replaced by Mg(II). In these (and the earlier) calculations, neither the C_2-acetyl nor C_{10a}-carbomethoxy group was explicitly included. These groups were treated as point masses of 15 amu, as were the ethyl and methyl substituents on the ring.

III. Results

The absorption spectrum of RC's from *Rb. sphaeroides* 2.4.1 in the 300–900-nm region is shown in Figure 3. The principal contributors to the different absorption bands are indicated in the figure. The various exciting lines used to probe the quinone-reduced RC's are indicated by the arrows. The high-frequency regions of the RR spectra of these RC's obtained at selected excitation wavelengths in near-infrared–red, orange–green, and violet–UV regions of the absorption spectrum are shown in Figures 4, 5, and 6, respectively. The spectra shown in the figures were

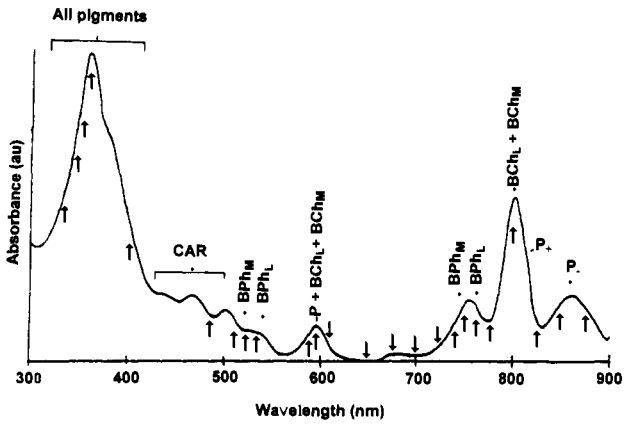

Figure 3. Electronic absorption spectrum of RC's from *Rb. sphaeroides* 2.4.1 at room temperature. The cofactors contributing to the various absorptions are indicated. The upper and lower excitonic components of P are labeled as P_+ and P_-, respectively. The arrows mark the different excitation wavelengths used to acquire RR spectra.

chosen because they exhibit all of the relevant vibrational features. The spectra obtained at the other excitation wavelengths indicated by the arrows in Figure 3 (not shown) do not reveal any new features. The relative intensities of the RR bands are, however, different at these other excitation wavelengths. RR spectra were also obtained for quinone-reduced RC's from the carotenoidless mutant *Rb. sphaeroides* R-26 (not shown) by using selected excitation wavelengths in the UV (363.8 nm), violet (406.7 nm), and green (530.9 nm) regions of the absorption spectrum. At these excitation wavelengths, the 1515–1540-cm^{-1} region of the RR spectra of the BCh's and BPh's in wild-type RC's is obscured by strong scattering from the CAR.[17a,c,37,38]

The high-frequency regions of the RR spectra of chemically oxidized RC's (P oxidized) obtained at selected excitation wavelengths in the near-infrared–red, orange, and violet–UV regions of the absorption spectrum are shown in Figures 7, 8, and 9, respectively. RR spectra of oxidized RC's were also obtained at several other excitation wavelengths (not shown); however, spectra were not acquired at all of the excitation wavelengths used to examine the quinone-reduced species. The spectra obtained do not represent a comprehensive set of data which exhibits all of the vibrational features of the oxidized protein. These spectra are presented in order to illustrate the effects of oxidation on the RR features of the different pigments in the RC. This will be discussed in more detail below.

The RR bands of quinone-reduced RC's observed at the various excitation wavelengths represented in Figures 4–6 are listed in Table I. The pigment affiliations of these bands are also indicated in the table (P, BCh, BPh, CAR). At certain excitation wavelengths, more than one type of pigment may contribute to the RR band contour. In such cases, the most plausible contributors are listed. If the L- and M-side affiliation is not specifically indicated, then either both pigments contribute to the RR band contour or the pigment affiliation is uncertain.

The RR bands assignable to fundamental carbonyl and skeletal modes in the 1425–1750-cm^{-1} region are listed in Table II. A single frequency indicates that the bands for the L- and M-side pigments are coincident unless otherwise noted. Two frequencies in parentheses indicate that two bands are observed but the pigment affiliation is uncertain. The calculated frequencies and normal mode descriptions for the high-frequency stretching modes of BCh are also listed in Table II. Finally, it should be noted that

(34) (a) Funfschilling, J.; Williams, D. F. *Appl. Spectrosc.* **1976**, *30*, 443–446. (b) Shreve, A. P.; Cherepy, N. J.; Mathies, R. A. *Appl. Spectrosc.* **1992**, *46*, 707–711.

(35) (a) Warshel, A.; Karplus, M. *J. Am. Chem. Soc.* **1972**, *94*, 5612–5625. (b) Warshel, A.; Levitt, M. *Quantum Chemistry Program Exchange*, No. 247, Indiana University, 1974.

(36) Donohoe, R. J.; Frank, H. A.; Bocian, D. F. *Photochem. Photobiol.* **1988**, *48*, 531–537.

(37) (a) Lutz, M.; Kleo, J.; Reiss-Husson, F. *Biochem. Biophys. Res. Commun.* **1976**, *69*, 711–717. (b) Lutz, M.; Agalidis, I.; Hervo, G.; Cogdell, R. J.; Reiss-Husson, F. *Biochim. Biophys. Acta* **1978**, *503*, 278–303. (c) Lutz, M.; Szponarski, W.; Berger, G.; Robert, B.; Neumann, J.-M. *Biochim. Biophys. Acta* **1988**, *894*, 423–433.

(38) (a) Koyama, Y.; Kito, M.; Takii, T.; Saiki, K.; Tsukida, K.; Yamashita, J. *Biochim. Biophys. Acta* **1982**, *680*, 109–118. (b) Koyama, Y.; Takii, T.; Saiki, K.; Tsukida, K. *Photobiochem. Photobiophys.* **1983**, *5*, 139–150.

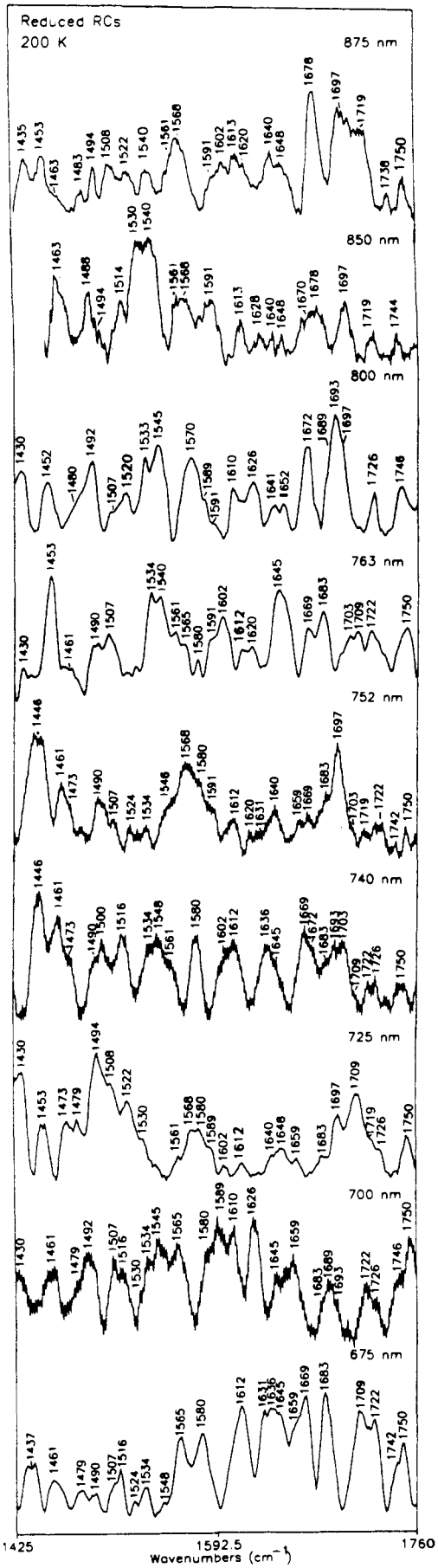

Figure 4. High-frequency regions of the RR spectra of quinone-reduced RC's from *Rb. sphaeroides* 2.4.1 at 200 K with excitation wavelengths in the near-infrared–red region. The relative intensities of the spectra are scaled for pictorial clarity.

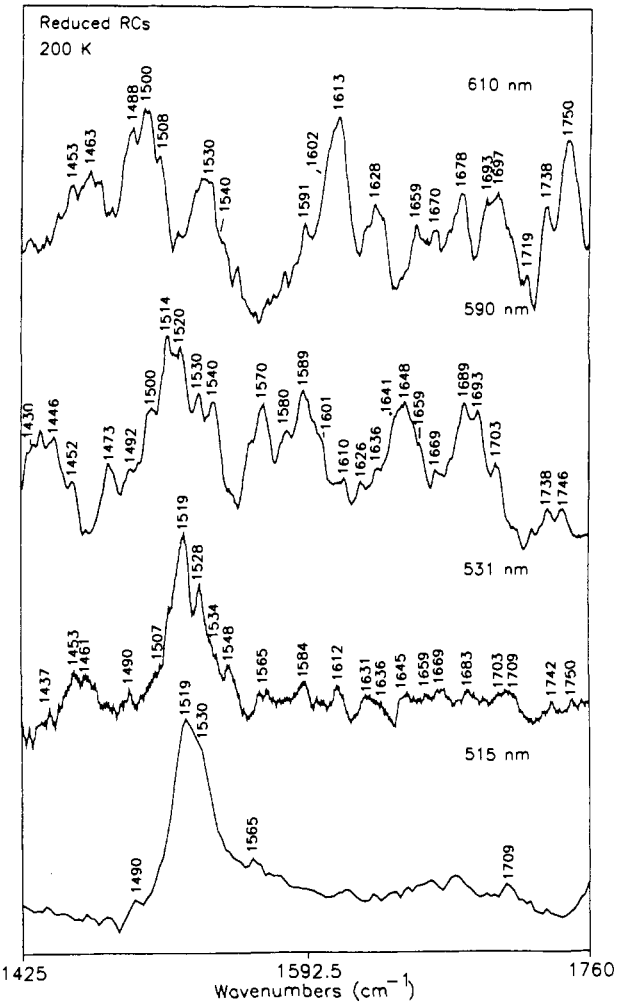

Figure 5. High-frequency regions of the RR spectra of quinone-reduced RC's from *Rb. sphaeroides* 2.4.1 at 200 K with excitation wavelengths in the orange–green region. The relative intensities of the spectra are scaled for pictorial clarity.

the vibrational assignments of certain skeletal modes of BCh listed in Table II are somewhat different than those we have previously proposed.[36] The revised assignments reflect the RR data reported herein for RC's and new RR data acquired for BCh and BPh in solution (P. C. Martin and D. F. Bocian, unpublished results).

The assignments for several nonskeletal and nonfundamental vibrations are listed in Table III. The nonskeletal vibrations are assigned as hydrogen bending fundamentals of the peripheral substituents on the bacteriochlorin rings. The nonfundamental modes are assigned as combination bands rather than overtones because no strong RR bands are observed at the appropriate fundamental frequencies. Because the bacteriochlorin pigments have a large number of normal modes, there are a variety of combinations that give frequencies commensurate with those listed in Table III. Consequently, it is not possible to assign a particular band to a specific binary combination.

IV. Discussion

A. General Features of the RR Spectra. The RR spectra of the quinone-reduced RC's exhibit a rich band structure in the 1425–1750-cm^{-1} region at all excitation wavelengths used in our studies. The RR spectra of oxidized RC's are also quite rich; however, these spectra bleach at certain excitation wavelengths (vide infra). The strong RR scattering observed for RC's upon excitation throughout the B- and Q-state absorptions is consistent with the results of RR studies on BCh, BPh, and other bacteriochlorin model complexes in solution.[17,19a,24,36] As the

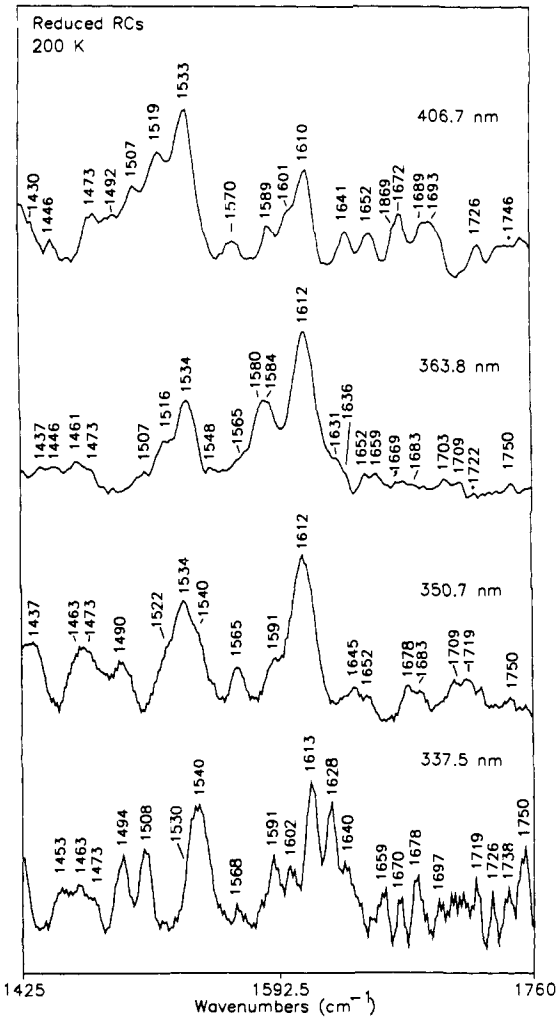

Figure 6. High-frequency regions of the RR spectra of quinone-reduced RC's from *Rb. sphaeroides* 2.4.1 at 200 K with excitation wavelengths in the violet–UV region. The relative intensities of the spectra are scaled for pictorial clarity.

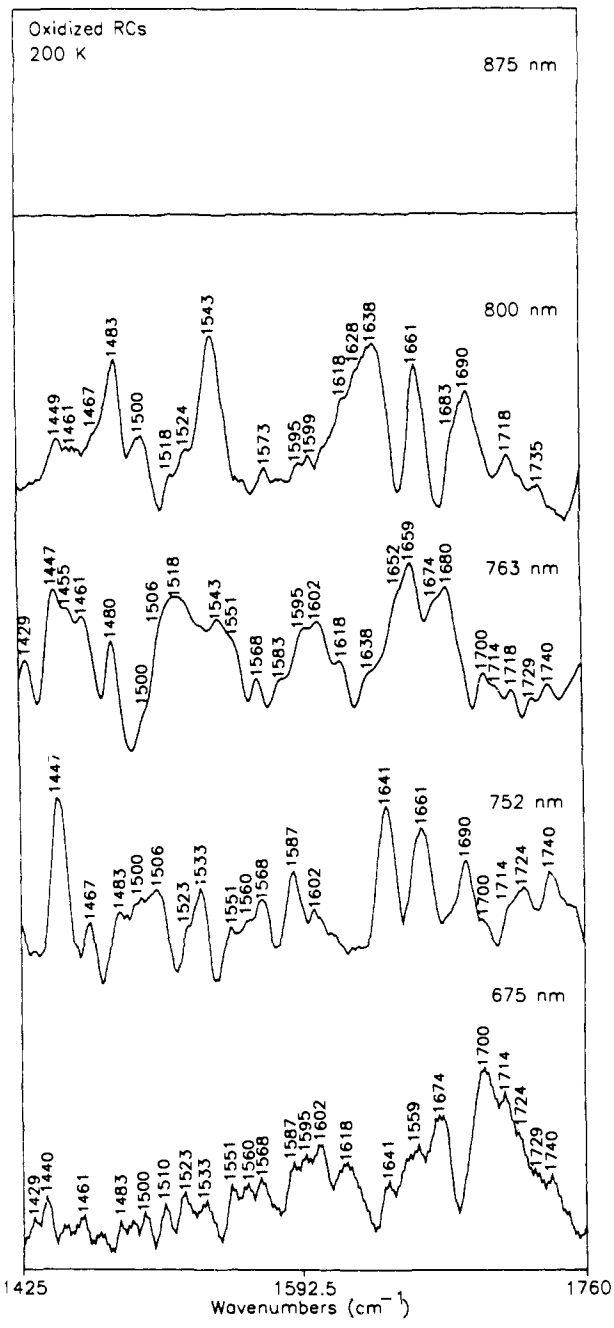

Figure 7. High-frequency regions of the RR spectra of oxidized RC's from *Rb. sphaeroides* 2.4.1 at 200 K with excitation wavelengths in the near-infrared–red region. The relative intensities of the spectra are scaled for pictorial clarity; however, the relative intensities of the 800- and 875-nm spectra are the same as those of the analogous spectra shown in Figure 4.

excitation wavelength is tuned throughout the different absorption bands of the various pigments in the RC's, the RR features gain and lose intensity with respect to one another. However, the overall pattern of resonance enhancement is extremely complicated, particularly in the region of overlapping absorptions from the different pigments. The complicated nature of the RR enhancement pattern most likely precludes any rigorous analysis. Any such analysis would require that RR spectra be acquired at very fine excitation intervals.

The complicated nature of the RR spectra of RC's is due to the fact that there are six pigments, each having at least four principal absorption bands (B_x, B_y, Q_x, Q_y) in the 335–875-nm region. There may also be charge-transfer bands of P in this spectral region.[5,6,12h,14f,39–41] Although the four principal absorption bands of a given pigment are energetically well separated, there is considerable overlap of analogous absorption bands of different pigments. This is illustrated in Figure 10, which shows a schematic representation of the absorption spectrum in the 475–900-nm region. The arrows in the figure represent the various exciting lines used in the RR studies. The stick spectrum indicates the approximate energies of the $Q_y(0,0)$, $Q_y(1,0)$, $Q_x(0,0)$, and $Q_x(1,0)$ absorptions of the six bacteriochlorin pigments in the RC. The Q_y-bands of P are designated by P_+ and P_-. The vibronic satellites of all the absorptions are placed $\sim$1500 cm^{-1} from the system origin, which is approximately where these bands occur for BCh's and BPh's in solution.[42] The stick spectrum is not meant to be an exact representation of the absorption spectrum of RC's (indeed, the exact positions of certain absorptions are not known, for example, the charge-transfer states of P) but rather is meant to provide a general picture of where the known absorptions of the six pigments lie relative to the various exciting lines used in the RR experiments. Likewise, the relative intensities shown in the stick spectrum are not necessarily indicative of the actual intensities but rather are drawn for pictorial clarity.

(39) (a) Warshel, A.; Parson, W. W. *J. Am. Chem. Soc.* **1987**, *109*, 6143–6152. (b) Parson, W. W.; Warshel, A. *J. Am. Chem. Soc.* **1987**, *109*, 6152–6163.

(40) (a) Thompson, M. A.; Zerner, M. C.; Fajer, J. *J. Phys. Chem.* **1990**, *94*, 3820–3828. (b) Thompson, M. A.; Zerner, M. C. *J. Am. Chem. Soc.* **1991**, *113*, 8210–8215.

(41) Scherer, P. O. J.; Fischer, S. F. In *Chlorophylls*; Scheer, H., Ed.; CRC Press: Boca Raton, FL, 1991; pp 1079–1093.

(42) Hoff, A. J.; Amesz, J. In *Chlorophylls*; Scheer, H., Ed.; CRC Press: Boca Raton, FL, 1991; pp 723–738.

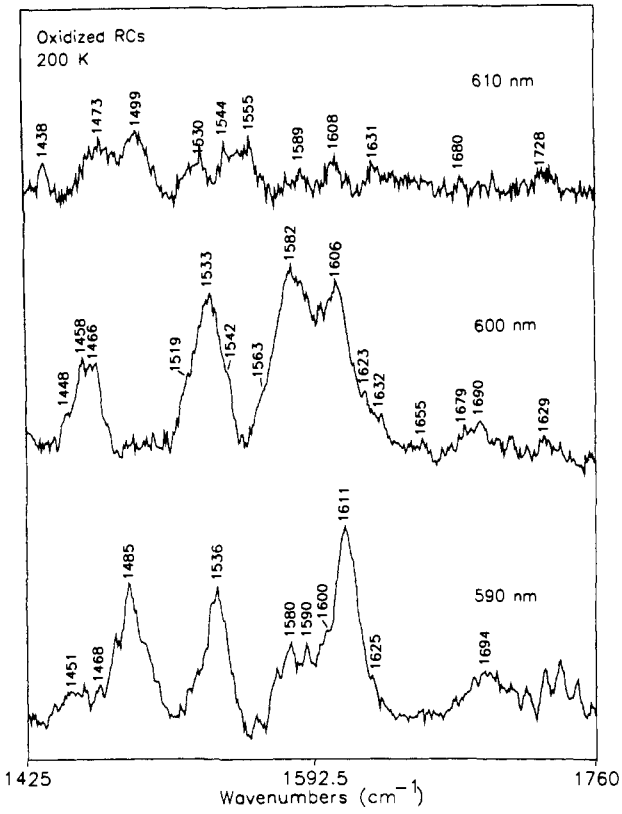

Figure 8. High-frequency regions of the RR spectra of oxidized RC's from *Rb. sphaeroides* 2.4.1 at 200 K with excitation wavelengths in the orange region. The relative intensities of the spectra are scaled for pictorial clarity; however, the relative intensity of the 610-nm spectrum is the same as that of the analogous spectrum shown in Figure 5.

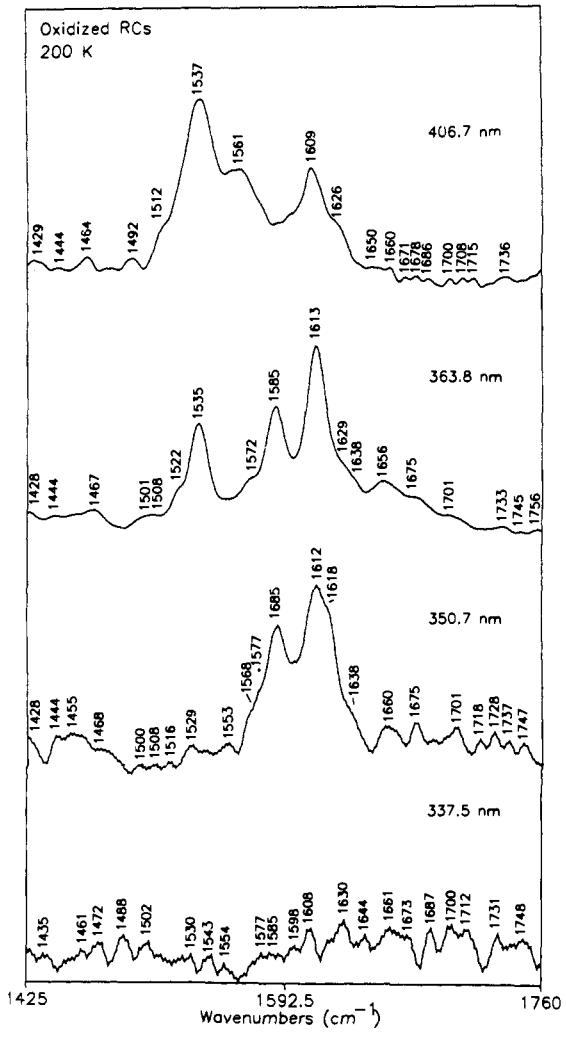

Figure 9. High-frequency regions of the RR spectra of oxidized RC's from *Rb. sphaeroides* 2.4.1 at 200 K with excitation wavelengths in the violet–UV region. The relative intensities of the spectra are scaled for pictorial clarity; however, the relative intensity of the 337.5-nm spectrum is the same as that of the analogous spectrum shown in Figure 6.

RR scattering from the vibronic satellites of the individual absorptions must be considered in analyzing the spectra of the different pigments in the RC's. The energetic offset of these bands from the system origin (typically 1200–1500 cm^{-1}) is such that the (1,0)-satellites from certain absorptions of one type of pigment fall in the range of the (0,0)-absorptions of another (Figure 10). For example, the $Q_y(1,0)$ bands of the accessory BCh's lie between the $Q_y(0,0)$ and $Q_y(1,0)$ absorptions of the BPh's; the $Q_x(1,0)$ bands of both P and the accessory BCh's lie near the $Q_x(0,0)$ bands of the BPh's. Although the vibronic satellites are weak (because the high-frequency and other modes of tetrapyrroles are typically weakly coupled to the electronic transitions), these states exhibit strong RR scattering.[43] In the small displacement limit, the RR intensity observed upon excitation into the strong (0,0)-absorption is equal to that observed upon excitation into the weak (1,0)-satellite.[44] This intensity enhancement pattern is maintained for both Franck–Condon (A-term) and Herzberg–Teller (B-term) scattering and has been experimentally verified in numerous RR studies of tetrapyrroles.[43] [In the case of RC's, certain low-frequency modes of P are known to be very strongly coupled to the lowest energy electronic transition.[6,14e,28d,31,45,46] This will influence the RR cross sections of the weakly coupled high-frequency modes and alter the RR enhancement pattern.[44]] The added complication of vibronic scattering dictates that extreme care must be exercised in the analysis of the RR spectra of RC's. This point has not been adequately appreciated in most previous RR studies of these systems.

Despite the considerable overlap of the absorption bands of the different pigments in RC's, it is possible to obtain a reasonable degree of selectivity for the different pigment types (P, accessory BCh's, and BPh's) through the appropriate choice of exciting lines. On the other hand, the close proximity of the absorptions of the analogous pigments on the L- versus M-sides renders selective excitation of these species impossible. In the sections below, we describe the general features of the RR spectra obtained with excitation in specific regions of the absorption spectrum. The discussion highlights absorption regions where substantial selectivity can be achieved for the different pigment types in the RC.

1. Quinone-Reduced RC's. a. Q_y-State-Excitation RR Spectra. The long-wavelength band of P is relatively isolated from the other strong absorptions of the protein (Figures 3 and 10); consequently, the RR spectra obtained with λ_{ex} = 875 nm are exclusively from P.[28c,d] This is confirmed by the disappearance of RR scattering upon bleaching of the absorption band via chemical oxidation (cf. Figures 4 and 7). In general, the RR spectrum of P observed with λ_{ex} = 875 nm is similar to Q_y-excitation RR spectra of BCh model compounds and preresonance Raman spectra of BCh.[19,30,36] With λ_{ex} = 850 nm, on the blue side of the long-wavelength absorption of P, several new RR bands are observed. These bands are also due to P (vide infra)

(43) Shelnutt, J. A. *J. Chem. Phys.* **1980**, *74*, 6644–6657 and references therein.

(44) Myers, A. B.; Mathies, R. A. In *Biological Applications of Raman Spectroscopy*; Spiro, T. G., Ed.; Wiley: New York, 1987; Vol. 2, pp 1–58.

(45) (a) Johnson, S. G.; Tang, D.; Jankowiak, R.; Hayes, J. M.; Small, G. J.; Tiede, D. M. *J. Phys. Chem.* **1989**, *93*, 5953–5957. (b) Johnson, S. G.; Tang, D.; Jankowiak, R.; Hayes, J. M.; Small, G. J.; Tiede, D. M. *J. Phys. Chem.* **1990**, *94*, 5849–5855. (c) Reddy, N. R. S.; Kolaczkowski, S. V.; Small, G. J. *Science* **1993**, *260*, 68–71.

(46) Klevanik, A. V.; Ganago, A. O.; Shkuropatov, A. Y.; Shuvalov, V. A. *FEBS Lett.* **1988**, *237*, 61–64.

Table I. RR Bands (cm^{-1}) of RC's Observed at Selected Excitation Wavelengths

excitation wavelength (nm)																
875	850	800	763	753	740	725	700	676	610	590	531	406.7	363.8	350.7	337.5	pigment[a]
1750									1750						1750	P_M
			1750	1750	1750	1750	1750	1750			1750		1750	1750		BPh
		1746				1746(sh)[b]	1746			1746		1746				BCh
	1744															P_M
			1742(sh)	1742(w)[b]				1742(sh)			1742					BPh
1738									1738	1738					1738	P_L
		1726			1726	1726(sh)	1726					1726			1726	BCh
			1722	1722	1722		1722	1722					1722(w)			BPh
1719	1719			1719(w)		1719(sh)			1719(w)					1719	1719	P
			1709		1709(sh)	1709		1709			1709		1709	1709		BPh_M
			1703	1703(sh)	1703				1703(sh)	1703	1703(sh)		1703			BPh_M
1697	1697	1697(sh)	1697(sh)	1697		1697			1697						1697	P_L
		1693			1693		1693(sh)		1693(sh)	1693		1693				BCh
		1689(sh)					1689			1689		1689				BCh
			1683	1683(sh)	1683(sh)	1683(sh)	1683(sh)	1683			1683		1683(w)	1683		BPh_L
1678	1678								1678					1678	1678	P_M
		1672			1672(sh)							1672				BCh
1670(sh)	1670								1670						1670	P_M
		1669(sh)								1669(w)		1669(sh)				BCh
			1669	1669	1669			1669			1669		1669(w)			BPh
			1659(sh)	1659	1659(sh)	1659	1659	1659(sh)			1659(w)		1659			BPh
1659(sh)									1659	1659(sh)					1659	P_M
													1652	1652		BPh
		1652					1652(sh)					1652				BCh
1648	1648					1648				1648						P_M
			1645		1645		1645	1645			1645			1645		BPh
		1641								1641		1641				BCh
1640	1640			1640		1640									1640	P_L
					1636			1636		1636(sh)	1636		1636(sh)			BPh_L
				1631(sh)				1631			1631		1631			BPh_M
	1628								1628						1628	P_M
		1626					1626		1626(sh)	1626(w)						BCh
1620			1620	1620												P_L
1613	1613								1613						1613	P
			1612	1612	1612	1612								1612		BPh, P
								1612			1612		1612			BPh
		1610					1610			1610(w)		1610				BCh
1602									1602(sh)						1602	P
			1602	1602(sh)	1602	1602								1602(sh)		BPh, P
								1602(sh)					1602(sh)			BPh
										1601(sh)		1601				BCh
1591	1591	1591(sh)	1591	1591					1591					1591	1591	P
		1589(sh)				1589	1589			1589		1589				BCh
								1584(sh)			1584		1584			BPh_M
			1580	1580(sh)	1580	1580	1580	1580		1580(sh)	1580(sh)		1580			BPh_L
		1570								1570		1570				BCh
1568	1568			1568		1568									1568(w)	P
			1565(sh)				1565	1565			1565		1565(sh)	1565		BPh
1561	1561		1561		1561(sh)	1561(sh)										P
				1548(sh)	1548			1548(w)	1548(w)		1548		1548(w)			BPh
		1545					1545									BCh
1540	1540		1540						1540(sh)	1540				1540(sh)	1540	P
			1534	1534	1534	1534(sh)	1534	1534			1534(sh)					BPh
											1528		1534	1534		CAR, BPh
		1533										1533				CAR, BCh
	1530					1530(sh)	1530(sh)		1530	1530					1530(sh)	P
			1524(w)	1524				1524(w)								BPh
1522						1522			1522(sh)					1522(sh)		P
		1520								1520						BCh
											1519	1519	1519(sh)			CAR
					1516		1516	1516			1516(sh)	1516(sh)	1516(sh)			BPh
	1514									1514						P
1508	1508(sh)					1508			1508						1508	P
								1507(sh)			1507(sh)		1507(sh)			BPh
		1507(sh)										1507				BCh
			1507	1507			1507									BPh, BCh
					1500				1500	1500						P
1494	1494(sh)					1494									1494	P
		1492					1492			1492(sh)		1492(w)				BCh
			1490	1490	1490	1490(sh)		1490			1490			1490		BPh
	1488								1488							P
1483																P
		1480(sh)														BCh
						1479	1479(sh)	1479								BPh
				1473(sh)	1473(sh)	1473				1473		1473(sh)	1473	1473	1473(sh)	BPh, BCh, P
1463(sh)	1463								1463					1463	1463	P
	c		1461(sh)	1461	1461		1461	1461			1461	1461	1461			BPh, BCh
1453	*c*		1453			1453			1453		1453				1453	P
	c	1452								1452						BCh
	c			1446	1446					1446		1446	1446			BPh
	c		1437(w)					1437			1437		1437	1437		BPh
	c	1430	1430			1430	1430			1430		1430				BCh

[a] At certain excitation wavelengths, more than one type of pigment (P, BCh, BPh, CAR) may contribute to the RR band contour. In such cases, the most plausible contributors are listed. If the L- and M-side affiliation is not specifically indicated, then either both pigments contribute to the RR band contour or the pigment affiliation is uncertain. [b] sh = shoulder; w = weak. [c] RR data not acquired in this spectral region with λ_{ex} = 850 nm.

Table II. Fundamental RR Bands (cm^{-1}) Assignable to Carbonyl and Skeletal Modes[a]

BPh_L	BPh_M	BCh_L and BCh_M	P_L	P_M	calc	assignment[b]
	(1750, 1742)	1746	1738	(1750, 1744)[c]	*d*	$\nu C_{10a}{=}O$
1683	(1709, 1703)[c]	(1693, 1689)	1697	1678	1701	$\nu C_9{=}O$
	(1669, 1659)	(1672, 1669)	1620?	(1670, 1659)[c]	*d*	$\nu C_{2a}{=}O$
	1645	1641		1640	1645	$\nu C_aC_m(\gamma)$, $\nu C_9{=}O$
1636	1631[e]	1626		1628	1627	$\nu C_bC_b(III)$, $\nu C_aC_m(\gamma)$
	1612	1610		1613	1612	$\nu C_aC_m(\alpha,\beta,\gamma,\delta)$
	1602	1601		1602	1593	$\nu C_aC_m(\delta)$, $\nu C_bC_b(I)$
1580	1584[f]	1589		1591	1586	$\nu C_bC_b(I)$, $\nu C_aC_b(III)$
	1565	1570		(1568, 1561)	1583	$\nu C_aC_m(\alpha,\delta)$, $\nu C_aC_b(I)$
	1534	1545		1540	1573	$\nu C_aC_m(\alpha,\beta,\delta)$
	1524	1533		1530	1523	$\nu C_aC_m(\alpha,\beta,\gamma,\delta)$, $\nu C_aN(I,II,IV)$
	1516	1520		(1522, 1514)	1514	$\nu C_aC_b(III)$, $\nu C_aN(I)$
	1507	1507		(1508, 1500)	1484	$\nu C_aN(II,IV)$, $\nu C_aC_b(I)$
	1490	1492		(1494, 1488)	1488	$\nu C_aC_b(I)$, $\nu C_aC_m(\beta)$, $\nu C_aN(II,IV)$
	1446	1452		1453	1463	$\nu C_aC_m(\alpha,\beta,\gamma)$
	1437	1430		1435	1430	$\nu C_aC_b(I,II,III,IV)$

[a] A single frequency indicates that the bands for the L- and M-side pigments are coincident unless otherwise noted; two frequencies in parenthesis indicate two bands are observed but the pigment affiliation is uncertain. [b] C_a, C_b, C_m, α, β, γ, and δ refer to the macrocycle positions shown in Figure 2. [c] Multiple bands are observed for this pigment (see text). [d] Frequency not calculated (see text). [e] Assignment of bands in this region to the L- and M-side pigments was taken from ref 17c (see text). [f] Assignment of bands in this region to the L- and M-side pigments was taken from ref 13a,b (see text).

Table III. Nonskeletal and Nonfundamental RR Bands (cm^{-1})

BPh	BCh	P	assignment
1722	1726	1719	combination
1652	1652	1648	combination
1548			combination
1479	1480	1483	combination
1461	1461	1463	ethyl CH_2 bend
1455			methyl CH_3 bend

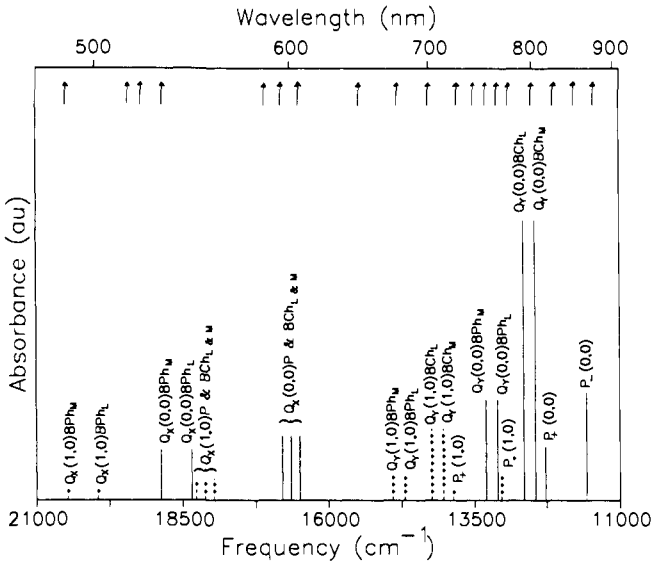

Figure 10. Schematic representation of the absorption spectrum of RC's in the 475–900-nm region. The solid and dashed lines indicate the approximate positions of the (0,0)-absorptions and (1,0)-vibronic satellites, respectively. The vibronic satellites of all the absorptions are placed ~1500 cm^{-1} from the system origin. The positions and relative intensities of the stick bands are not meant to be exact but rather to give a general picture of the various absorptions of the six pigments in the RC. The absorptions of the CAR are not shown. The arrows mark the different excitation wavelengths used to acquire RR spectra in this region.

and include features at 1488, 1514, and 1561 cm^{-1}. As the excitation wavelength is tuned closer to the $Q_y(0,0)$ absorptions of the accessory BCh's, the new spectral features observed with λ_{ex} = 850 nm, as well as other features attributable to P (for example, bands at 1719, 1697, and 1678 cm^{-1}) decrease in intensity. With λ_{ex} = 800 nm, no RR features due to P are observed and the spectrum is dominated by scattering from the accessory BCh's. In general, the spectra of the accessory BCh's are similar to those of P and BCh in solution.[17,19,24,30,36]

The RR spectra observed with λ_{ex} in the 700–780-nm range are extremely complicated. This region includes the $Q_y(0,0)$ absorptions of the BPh's as well as vibronic satellites from P and the accessory BCh's (Figure 10). Features attributable to the BPh's are clearly observed in the RR spectra obtained in this region. These include bands in the 1703–1709- and 1580–1585-cm^{-1} ranges.[17] However, scattering is also observed from P and the accessory BCh's. This is illustrated by the appearance of bands at 1697 cm^{-1} (P) and 1693 cm^{-1} (BCh's). The RR scattering from P and the accessory BCh's is due to resonance with the vibronic satellites of the red absorptions of these pigments. The RR bands of P observed with λ_e = 700–780 nm can be eliminated via chemical oxidation (cf. Figures 4 and 7). However, it must be emphasized that the formation of P^+ not only eliminates RR scattering from the P but also alters the RR spectra of the accessory BCh's and the BPh's (cf. Figures 4–6 and 7–9). As a consequence, the correlation of the RR bands of these latter pigments in quinone-reduced versus oxidized RC's is not straightforward. This will be discussed further in Section IV.A.2.

The $Q_y(1,0)$ bands of the BPh's are relatively isolated from the other absorptions of the Q_y envelope (Figures 3 and 10); consequently, these pigments scatter exclusively with λ_{ex} = 675 nm.[28c] This is confirmed by the observation of RR bands characteristic of BPh, such as the modes near 1709 and 1580 cm^{-1}, and the absence of bands characteristic of P or the accessory BCh's, such as modes near 1697 (P), 1693 (accessory BCh's), 1590 (P and accessory BCh's), and 1540 cm^{-1} (P and accessory BCh's) (Figure 4: cf. λ_{ex} = 875 and 675 nm; λ_{ex} = 800 and 675 nm). Overall, the RR spectra of the BPh's in the protein are similar to those of BPh in solution.[17]

b. Q_x-State-Excitation RR Spectra. The Q_x bands of P and the accessory BCh's are strongly overlapped near 600 nm (Figures 3 and 10); consequently, RR scattering is observed from both of these pigment types upon excitation in this region. The bands of P dominate with excitation on the red side of the band contour. This is illustrated by comparison of the RR spectra obtained with λ_{ex} = 610 versus 590 nm (Figure 5). With the longer wavelength excitation, the 1697- and 1678-cm^{-1} bands of P are clearly observed; these bands are absent from the spectra obtained with the shorter excitation wavelength. At the shorter excitation wavelength, bands characteristic of the accessory BCh's are observed, such as those at 1693 and 1689 cm^{-1}. The dominance of scattering by P on the red side of the Q_x bands is further exemplified by the strong decrease in RR intensity upon oxidation of P (cf. Figures 5 and 8).

The Q_x absorptions of the BPh's are in the 530–545-nm range and are reasonably well separated form those of P and the accessory BCh's (Figures 3 and 10). Excitation on the high-

energy side of this range produces exclusive scattering from the BPh's.[17] This is illustrated by the appearance of characteristic BPh bands, such as those in the 1703–1709-, 1631–1636-, and 1580–1585-cm^{-1} ranges, and the absence of any bands characteristic of P or the accessory BCh's. Excitation near 530 nm is closer to the $Q_x(0,0)$ absorption of BPh_M whereas excitation near 545 nm is closer to the $Q_x(0,0)$ absorption of BPh_L.[11,47] Excitation in these two different regions has previously been used to characterize scattering from the two different BPh's.[17c] While some selectivity is possible, we find that both BPh's contribute strongly to the RR scattering upon excitation in the 530–545-nm range. We also find that excitation on the longer wavelength side of the range results in scattering from P and/or the BCh's (not shown). This scattering arises from the vibronic satellites of the Q_x bands of these latter pigments (Figure 10). In wild-type RC's, scattering from the CAR is extremely strong with excitation throughout the 475–550-nm region. This gives rise to bands in the 1515–1540-cm^{-1} range.[17a,c,37,38] With λ_{ex} = 475–515 nm, only CAR scattering is observed (Figure 5).

c. **B-State-Excitation RR Spectra.** The B-state absorptions of all six pigments are strongly overlapped (Figure 3). However, previous RR studies have shown that excitation on the longer wavelength side of the B bands results in scattering primarily from the accessory BCh's whereas excitation near the band maximum gives rise to scattering primarily from the BPh's.[17,27] Indeed, comparison of Figures 4 and 6 reveals that the RR spectrum obtained with λ_{ex} = 406.7 nm exhibits features similar to those observed with λ_{ex} = 800 nm whereas the spectrum obtained with λ_{ex} = 363.8 nm exhibits features similar to those observed with λ_{ex} = 675 nm. Previous B-state-excitation RR studies have also shown that P contributes very little to the RR spectrum with excitation in the 350–420 nm region.[17,18,27] This is illustrated by the lack of significant bleaching of the RR signals upon oxidation of P (cf. Figures 6 and 9).

Because of the extensive overlap of the B-state absorptions of the different pigments in the RC, it is not obvious where scattering from P might make a strong contribution to the RR spectrum. In order to determine whether RR scattering from P could be observed with excitation in this region, we performed experiments with excitation on the short wavelength side of the B band(s). With λ_{ex} = 337.5 nm, the RR spectrum is significantly different from that observed with excitation at longer wavelengths (Figure 6). In particular, the RR spectrum exhibits features at 1719 and 1678 cm^{-1}. These features are characteristic of P (Figure 4) and are not observed with other UV and violet excitation wavelengths (Figure 6). Upon oxidation of P, the RR scattering observed with λ_{ex} = 337.5 nm is strongly attenuated (cf. Figures 6 and 9). Together, these observations suggest that the RR spectrum obtained at this excitation wavelength is dominated by scattering from P.

It is not clear which electronic absorption of P is responsible for the RR scattering observed with λ_{ex} = 337.5 nm. A possible candidate is the higher energy component of the coupled B_x transitions of the dimer. Both the B_x and B_y transitions are expected to be strongly coupled because these are relatively strong transitions in the monomer (unlike the Q-state transitions where Q_y is strong and Q_x is weak).[42] Presuming that the orientation of the transition dipoles of the B_x and B_y transitions are similar to those of the Q_x and Q_y transitions, respectively, the strongly allowed member of the B_y pair should be shifted to the red (as is the case for the Q_y transitions), whereas the strongly allowed member of the B_x pair should be shifted to the blue.[39-41] The red shift of the strongly allowed member of the y-polarized transitions is due to the fact that the constituent monomers of P are displaced with respect to one another such that the angle between the line of centers in the y-direction is greater than the magic angle.[8-10] [Here, we use the formalism of dipolar exciton coupling which is not strictly correct for P[39-41] but is sufficient for the present qualitative discussion.] In contrast, the angle between the line of centers in the x-direction is less than the magic angle,[8-10] which would lead to a blue shift of the strongly allowed member of the pair. Regardless of the exact origin of the RR scattering observed with λ_{ex} = 337.5 nm, it appears that additional information regarding the vibrational characteristics of P can be obtained via more extensive RR studies in this region.

2. **Oxidized RC's.** As was previously noted, the formation of P^+ alters the RR spectra of both the accessory BCh's and the BPh's. This is best illustrated via comparison of the RR spectra obtained with λ_{ex} = 800 (BCh) and 675 nm (BPh) for quinone-reduced (Figure 4) versus oxidized RC's (Figure 7). The oxidation-induced changes in the RR spectra of the accessory BCh's and BPh's include both frequency shifts and relative intensity changes. The combination of these effects precludes any straightforward correlation of the RR spectra of quinone-reduced and oxidized RC's. We have not yet acquired RR data of oxidized RC's at a sufficiently large number of wavelengths to obtain a detailed picture of the scattering characteristics or to make a complete set of vibrational assignments. Such a detailed RR study of oxidized RC's is currently in progress in our laboratory. The objective of this study is not only to characterize rigorously the effects of oxidation on the accessory BCh and BPh pigments but also to determine the most suitable excitation wavelengths for examining P^+. Finally, we emphasize that the oxidation-induced frequency shifts of certain vibrational modes of the accessory BCh's and BPh's are large (as much as 10 cm^{-1}).[28c] Accordingly, the spectral changes associated with these pigments must be considered in the interpretation of RR, IR, or time-resolved vibrational spectra which compare P and P^+.[13c,15,20,32] In most previous vibrational studies of RC's, this point has not been generally appreciated.

B. Vibrational Assignments. The vibrational assignments for the BCh and BPh pigments in the RC's were determined in a stepwise fashion. The first step was to globally examine the RR spectra obtained at all of the different excitation wavelengths. The spectra were then screened in order to determine the excitation wavelengths that give the most selective excitation of the different pigment types (vide supra). The criteria for determining selectivity included (1) the dominant contributor to the RR cross section as predicted by the absorption spectrum, (2) the observation of bleaching of the RR spectrum upon oxidation of P, and (3) the exclusive observation of characteristic RR features associated with BCh versus BPh as determined by studies of the pigments in solution.[17,19,24,30] The selected RR spectra of the RC's were then compared with one another and with those previously reported of a variety of porphyrin, chlorin, and bacteriochlorin model compounds.[24,25,48,49] The objective of these comparisons was to identify repeated elements among the spectra of the different pigments in the RC's and between the spectra of these pigments and those of the model compounds. The entire process was guided throughout by the predictions of normal coordinate calculations on BCh and on various model compounds.[36,48,49]

The final consideration in the assignment of the RR spectra of RC's concerns the identification of bands due to a given pigment type in the L- versus M-subunits. As was previously noted, some degree of selectivity can be achieved in the examination of the RR spectra of the L- versus M-side pigments; however, the

(47) Dutton, P. L.; Prince, R. C.; Tiede, D. M. *Photochem. Photobiol.* **1978**, *28*, 939–949.

(48) (a) Li, X.-Y.; Czernuszewicz, R. S.; Kincaid, J. R.; Su, Y. O.; Spiro, T. G. *J. Phys. Chem.* **1990**, *94*, 31–47. (b) Spiro, T. G.; Czernuszewicz, R. S.; Li, X.-Y. *Coord. Chem. Rev.* **1990**, *100*, 541–571. (c) Prendergast, K.; Spiro, T. G. *J. Phys. Chem.* **1991**, *95*, 9728–9736. (d) Melamed, D.; Sullivan, E. P., Jr.; Prendergast, K.; Strauss, S. H.; Spiro, T. G. *Inorg. Chem.* **1991**, *30*, 1308–1319.

(49) (a) Boldt, N. J.; Donohoe, R. J.; Birge, R. R.; Bocian, D. F. *J. Am. Chem. Soc.* **1987**, *109*, 2284–2298. (b) Procyk, A. D.; Bocian, D. F. *J. Am. Chem. Soc.* **1991**, *113*, 3765–3773. (c) Procyk, A. D.; Kim, Y.; Schmidt, E.; Fonda, H. N.; Chang, C.-K.; Babcock, G. T.; Bocian, D. F. *J. Am. Chem. Soc.* **1992**, *114*, 6539–6549. (d) Procyk, A. D.; Bocian, D. F. *Annu. Rev. Phys. Chem.* **1992**, *43*, 465–496.

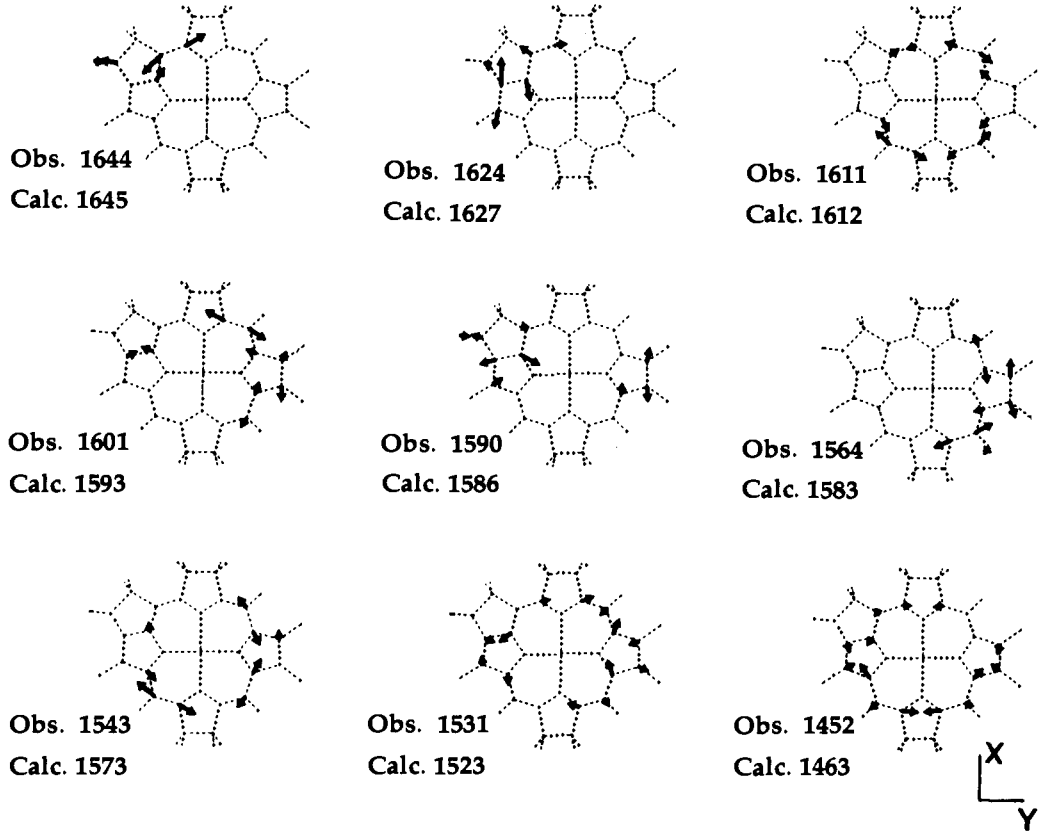

Figure 11. Vibrational eigenvectors of BCh which contain substantial contributions from C_aC_m and C_bC_b stretching motions. The listed observed frequencies are the averages of those observed for BCh and P in this study.

absorption bands are sufficiently overlapped that both pigments scatter at a given excitation wavelength. The complications due to vibronic scattering significantly compromise the use of relative RR intensities as indicators of subunit affiliation. The assignments are further complicated by the possibility that the RR bands of certain modes may be coincident for the L- versus M-side pigments whereas those of others may not. To aid in the vibrational assignments, we utilized X-ray crystallographic data[8c,9c,10c] and RR spectra from genetically modified RC's.[13a,b,28c] These data are most useful in the assignment of the carbonyl modes because they provide insights into the hydrogen bonding interactions that are possible between these groups and various protein residues. Before discussing the assignments for the individual pigments, it is useful to describe the general characteristics of the modes that are expected to contribute to the vibrational spectra in the 1425–1750-cm^{-1} range.

The first general class of modes that appear in the spectral range of interest are the carbonyl stretches ($\nu C{=}O$).[17] The modes of highest frequency are the $\nu C{=}O$ vibrations associated with the C_7-propionate and C_{10}-carbomethoxy groups. These modes lie in the 1730–1750-cm^{-1} range.[17d] The carbonyl associated with the propionate group is well removed from the π system of the macrocycle, and the $\nu C_{7c}{=}O$ vibration is not resonance enhanced in the Raman spectrum. The carbonyl associated with the C_{10}-carbomethoxy group is also removed from the π system of the ring; however, the $\nu C_{10a}{=}O$ mode does gain resonance enhancement in the Raman spectrum.[28a,50] The enhancement of this mode most likely occurs through kinematic coupling with skeletal modes of macrocycles (P. C. Martin and D. F. Bocian, unpublished results). The carbonyl stretches of the C_9-keto and C_2-acetyl groups lie at somewhat lower frequency (1630–1710 cm^{-1}). It is well established that both the $\nu C_9{=}O$ and $\nu C_{2a}{=}O$ modes are resonance enhanced in the Raman spectra of chlorin and bacteriochlorin pigments.[17-19,24,28a,36,49a,50,51]

The second general class of modes that appear in the spectral range of interest is the ring stretches associated with the methine bridges (νC_aC_m) and the β-bonds of the pyrrole rings (νC_bC_b).[36,48,49] The normal coordinate calculations predict that all eight νC_aC_m modes and the two νC_bC_b modes associated with rings I and III lie in the 1460–1640-cm^{-1} range (Table II; Figure 11). The νC_bC_b vibrations of the single β-bonds in rings II and IV lie at much lower frequencies and are out of the range of interest. The vibrational characteristics of the νC_aC_m and νC_bC_b modes are the focus of our discussion of the structural features of the BCh and BPh macrocycles. In this regard, Figure 11 illustrates the calculated vibrational eigenvectors for the nine skeletal modes that contain the largest amount of C_aC_m and C_bC_b stretching character. Displacements are shown only for those atoms whose motions contribute significantly to the normal mode (10% or greater of the maximum atomic displacement of a given mode). The observed frequencies listed in Figure 11 are the average values exhibited by P and the accessory BCh's in the RC's (Table II).

The best characterized skeletal vibration of bacteriochlorins is the νC_aC_m mode observed near 1611 cm^{-1} (Figures 4–6 and 11; Table II).[17,18,24,27,36] This vibration is the analog of the ν_{10}-mode of metalloporphyrins.[48a,b,49d] It has generally been assumed that the ν_{10} analog is the highest frequency skeletal vibration of BPh and BCh. However, the normal coordinate calculations predict that two other modes lie higher. One of these is the νC_aC_m vibration of the methine bridge associated with rings III and V, and the other is the νC_bC_b mode of ring III. The unusually high frequencies of these modes are due to strain introduced by the fusion of rings III and V and mixing with the $\nu C_9{=}O$ vibrations (Figure 11). The prediction that two skeletal modes lie higher in frequency than the ν_{10} analog prompted us to perform a detailed investigation of the RR spectra of BCh and BPh in solution (P.

(50) (a) Heald, R. L.; Callahan, P. M.; Cotton, T. M. *J. Phys. Chem.* **1988**, *92*, 4820–4824. (b) Heald, R. L.; Cotton, T. M. *J. Phys. Chem.* **1990**, *94*, 3968–3975.

(51) Perng, J.-H.; Bocian, D. F. *J. Phys. Chem.* **1992**, *96*, 10234–10240.

C. Martin and D. F. Bocian, unpublished results). These studies reveal that weak RR bands are observed in the 1620–1650-cm^{-1} spectral region which cannot be attributed to $\nu C{=}O$ vibrations. We have also observed such modes in the RR spectra of chlorophyll and chlorophyll model compounds.[49a,51] These modes have important implications for the vibrational assignments of RC's in the 1620–1660-cm^{-1} region (vide infra). The other six νC_aC_m vibrations and the remaining νC_bC_b modes are predicted to lie lower in frequency than the ν_{10} analog. However, several of these modes are clustered between 1590 and 1605 cm^{-1} (Table II, Figure 11).

The third general class of modes that appear in the spectral range of interest is vibrations associated with the C_aC_b and C_aN bonds. The normal coordinate calculations predict that these two mode types are, in general, extensively mixed with one another and, in some cases, with the νC_aC_m vibrations (Table II). The calculations predict that there are three $\nu C_aC_b/\nu C_aN$ modes in the 1425–1525-cm^{-1} regime. The highest frequency $\nu C_aC_b/\nu C_aN$ vibration (1514 cm^{-1}) involves ring III. The unusually high frequency for this mode again is due to strain introduced by the fusion of rings III and V.

The last general class of modes that appear in the spectral range of interest are nonfundamental vibrations and fundamental modes that are not associated with the carbonyl groups or ring skeleton (Table III). In this regard, RR studies of porphyrin and chlorin model compounds have shown that the CH deformations of the nonconjugating alkyl substituents are observed in the RR spectra in the 1460–1480-cm^{-1} range.[48,49] Finally, various combination and overtone bands are also observed in the RR spectra of model compounds throughout the spectral range of interest. These modes are generally weak; however, they must be considered in the vibrational analysis (vide infra).

In the following sections, we discuss the vibrational assignments for the carbonyl and skeletal modes of the various pigments in the RC's. We first discuss the accessory BCh's because the spectra of these pigments are the most straightforward to interpret. We then proceed to P. The assignment of the spectra of these pigments is more complicated than those of the accessory BCh's; however, the assignments obtained for the latter pigments provide a bridge to the discussion of the more complicated spectra of P. Finally, we discuss the assignments for the BPh's.

1. Accessory BCh's. The RR spectra of the accessory BCh's exhibit bands at 1746, 1726, 1693, 1672, 1652, 1641, and 1626 cm^{-1}, which are candidates for $\nu C{=}O$ vibrations. The 1746- and 1726-cm^{-1} bands are the only candidates for $\nu C_{10a}{=}O$ modes whereas the 1693- and 1672-cm^{-1} bands are the only reasonable possibilities for $\nu C_9{=}O$ vibrations. The 1672-, 1652-, 1641-, and 1626-cm^{-1} bands are all possibilities for $\nu C_{2a}{=}O$ vibrations. The X-ray crystallographic data for RC's from *Rb. sphaeroides* indicate that no hydrogen bonds exist between protein residues and the C_{10a}-carbomethoxy, C_9-keto, and C_2-acetyl carbonyl groups of the BCh's in both the L- and M-subunits (Figure 1). On the basis of these data, we assign the 1746-, 1693-, and 1672-cm^{-1} bands to the $\nu C_{10a}{=}O$, $\nu C_9{=}O$, and $\nu C_{2a}{=}O$ modes, respectively, of both BCh_L and BCh_M. Although these modes of the two pigments appear to be essentially coincident, the bands attributed to the $\nu C_9{=}O$ and $\nu C_{2a}{=}O$ vibrations both exhibit a slight splitting (1693 and 1689 cm^{-1}; 1672 and 1669 cm^{-1}; Figure 6, λ_{ex} = 406.7 nm). These splittings may be due to the L- versus M-side pigments; however, the splittings are so small that they could also be due to inhomogeneities. It should be noted that Lutz and co-workers have previously assigned bands near 1693 and 1672 cm^{-1} to the $\nu C_9{=}O$ and $\nu C_{2a}{=}O$ modes, respectively, of both BCh_L and BCh_M; thus, our assignments concur with theirs.[17c,d,18] The frequencies we observe for these modes are somewhat different from those reported by Lutz and co-workers; however, their values were obtained from P/P^+ difference RR experiments. In addition, these two sets of experiments were conducted at different temperatures.

The question remains as to the origin of the bands observed at 1726, 1652, 1641, and 1626 cm^{-1}. It is possible that these are also carbonyl modes; however, the frequencies of these modes, with the exception of the 1652-cm^{-1} band, are indicative of hydrogen-bonded species.[17,18] Hydrogen bonding is not consistent with the X-ray crystallographic data (Figure 1).[10c] Consequently, any hydrogen bonds that might exist would necessarily come from water. We do not believe that any of the remaining bands are due to $\nu C{=}O$ vibrations for the following reasons: (1) The basic pattern whereby bands are observed near 1725, 1652, 1641, and 1626 cm^{-1} occurs in the RR spectra of all three types of pigments (P, BCh's, BPh's) in the RC's (vide infra). Given that the hydrogen bonding is different among the various pigments, it seems unlikely that this consistent pattern would be repeated if the bands were due to $\nu C{=}O$ vibrations. (2) Examination of the RR spectra of BCh and BPh in solution reveals that weak RR bands are observed near both 1750 and 1725 cm^{-1} even in solvents that are not capable of hydrogen bonding (P. C. Martin and D. F. Bocian, unpublished results). As was previously noted, bands are also observed in the 1620–1650-cm^{-1} region of the RR spectra of BCh and BPh in solution which are not attributable to $\nu C{=}O$ modes. (3) The normal coordinate calculations predict that two skeletal modes lie in the 1620–1640-cm^{-1} region (Table II, Figure 11). Given these arguments, we assign the 1641- and 1626-cm^{-1} RR bands of the accessory BCh's to the two skeletal fundamentals. The bands due to BCh_L and BCh_M appear to be coincident.

Collectively, the assignments of the 1746-, 1693-, 1672-, 1641-, and 1626-cm^{-1} bands as carbonyl and skeletal fundamental modes of both BCh_L and BCh_M leave no option but to attribute the 1726- and 1652-cm^{-1} RR bands to nonfundamental vibrations (Table III). The assignment of the 1641- and 1626-cm^{-1} bands as skeletal fundamentals also brings the observed and calculated vibrational patterns for the remainder of the skeletal modes into near-perfect registry (Table II). In particular, no strong RR bands are observed for which there are not corresponding calculated modes. The calculations suggest that the RR bands observed at 1601, 1570, 1545, 1533, 1492, and 1452 cm^{-1} correspond to the six νC_aC_m modes that lie below the ν_{10} analog at 1610 cm^{-1} while the band observed at 1589 cm^{-1} corresponds to the remaining νC_bC_b vibration. The three RR bands observed at 1520, 1507, and 1430 cm^{-1} are attributed to $\nu C_aC_b/\nu C_aN$ vibrations. [The assignments for the 1507- and 1492-cm^{-1} RR bands are reversed from descending frequency order because the observed and calculated ^{15}N shifts are more consistent with the inverted order.[17a]] We assign the remaining weak bands observed in the RR spectra of the accessory BCh's near 1480 and 1460 cm^{-1} to nonskeletal or nonfundamental vibrations (Table III) by analogy to the spectra of model compounds.[48a,b,49a] Finally, it is important to note that, as is the case with the $\nu C{=}O$ modes of the accessory BCh's, the RR bands corresponding to analogous skeletal fundamentals of BCh_L and BCh_M appear to be nearly coincident. There is no evidence of doubling of any of the RR bands although certain bands are relatively broad, suggesting small frequency differences.

2. Special Pair BCh's. The RR spectra of P exhibit bands at 1750, 1744, 1738, 1719, 1697, 1678, 1670, 1659, 1648, 1640, 1628, and 1620 cm^{-1}, which are candidates for the $\nu C{=}O$ vibrations. The 1750-, 1744, 1738-, and 1719-cm^{-1} bands are the only possibilities for the $\nu C_{10a}{=}O$ modes. The 1697-, 1678-, 1670-, and 1659-cm^{-1} bands are candidates for the $\nu C_9{=}O$ vibrations while the remaining bands are candidates for the $\nu C_{2a}{=}O$ vibrations. The X-ray crystallographic data for RC's from *Rb. sphaeroides* indicate that no hydrogen bonds exist between protein residues and the C_{10}-carbomethoxy, C_9-keto, and C_2-acetyl carbonyl groups of P_M and the C_9-keto group of P_L (Figure 1).[10c] In contrast, both the C_{10a}-carbomethoxy and C_2-acetyl carbonyls of P_L are hydrogen bonded. On the basis of these data, we assign the 1750- and 1744-cm^{-1} bands to the $\nu C_{10a}{=}O$ mode of the free carbonyl of P_M and the 1738-cm^{-1} band to the hydrogen-bonded carbonyl of P_L. This latter

assignment is consistent with the results of FT-IR studies on RC's.[13c,17d,20] The two bands observed for the νC_{10a}=O mode of P_M suggest that there is some heterogeneity in the enviroment of this pigment (vide infra). [An alternative assigment is that one of the two bands is a nonfundamental mode unique to P.] We assign the 1697- and 1678-cm^{-1} bands as the νC_9=O modes of the free carbonyls of P. In this regard, Lutz and co-workers have previously assigned bands in this region to P_L and P_M, respectively, on the basis of P/P^+ difference RR experiments.[17c,d,18] In contrast, the reverse assignment has been suggested by workers performing FT-IR studies on genetically modified RC's.[13c] We have no clear basis for choosing between the two different assignments and have retained the assignment proposed by Lutz and co-workers in Table II. Regardless of the correct assignments for the νC_9=O modes of P_L and P_M, there are no protein residues which are capable of hydrogen bonding to these carbonyl groups (Figure 1) and it is not obvious why the frequencies of the two modes are so different. However, it is possible that the frequency difference reflects a difference in the local dielectric constant of the medium surrounding P_L versus P_M. In this regard, Krawczyk has shown that the frequency of the νC_9=O vibration of chlorophyll *a* in aprotic solvents is significantly influenced by dielectric effects.[52] The frequency of this mode downshifts as the dielectric constant of the solvent increases.

The assignment of the νC_{2a}=O modes of P is problematic. In particular, bands are observed at 1670, 1659, and 1648 cm^{-1} which could be attributed to the νC_{2a}=O mode of the free carbonyl of P_M. Lutz and co-workers have previously assigned a band near 1650 cm^{-1} to this mode.[17c,d,18] However, we believe that a more consistent assignment for the 1648-cm^{-1} band is as a nonfundamental mode whose analog is observed at 1652 cm^{-1} in the case of the accessory BCh's (Table III). We are not certain which one of the remaining two bands (1670 and 1659 cm^{-1}) is the M-side νC_{2a}=O mode. It is possible that both bands are due to this vibration. This would be consistent with heterogeneity in the environment of P_M as is also implied by the doubling of the νC_{10a}=O mode of this pigment (vide supra). In the case of the L-side acetyl carbonyl, the RR spectrum is extremely congested in the region where a band due to a hydrogen-bonded carbonyl group would be expected (1620–1640-cm^{-1}). On the basis of P/P^+ difference RR and FT-IR experiments, previous workers have assigned a weak band in the 1620–1630-cm^{-1} region to this mode.[13c,17c,d,18] However, bands in this spectral region are also characteristic of ring skeletal modes (Table II, Figure 11). In particular, the 1640- and 1626-cm^{-1} bands of P would seem to be best attributed to skeletal fundamentals (rather than carbonyl modes) by analogy to the assignments for the accessory BCh's. We do observe a weak band near 1620 cm^{-1} which does not appear in the RR spectra of the accessory BCh's and which does not clearly correspond to a ring skeletal mode. We tentatively assign this band as the νC_{2a}=O mode of P_L. Finally, we attribute the remaining RR band of P at 1719 cm^{-1} to a nonfundamental mode whose analog is observed at 1726 cm^{-1} in the spectra of the accessory BCh's.

In the 1540–1620-cm^{-1} region of the RR spectra, there is a one-to-one correspondence between the RR bands exhibited by P and the BCh's. One possible exception is an apparent doubling of the band near 1565 cm^{-1} (Figure 4, λ_{ex} = 850 nm). In the 1480–1540-cm^{-1} region, the spectra of P and the accessory BCh's are different. Although the spectra of P exhibit bands at 1522, 1508, and 1494 cm^{-1} which appear to be the analogs of the 1520-, 1507-, and 1492-cm^{-1} bands of the accessory BCh's, a second series of bands is also observed at 1514, 1500, and 1488 cm^{-1} (Figure 4, λ_{ex} = 850; Figure 5, λ_{ex} = 610 nm). This type of band pattern is not observed in the RR spectra of BCh in solution at any excitation wavelength we have used to probe the pigment (P. C. Martin and D. F. Bocian, unpublished results). In addition, the bands in the second series are reasonably strong and it seems unlikely that they are due to nonfundamental modes. Accordingly, we have assigned the two different sets of bands to the two different pigments in P. However, the pigment affiliation of the two sets of bands is not clear (Table II). The X-ray crystallographic data available for RC's do not provide any clear insights that might aid in the assignment (vide infra).

3. BPh's. The RR spectra of the BPh's exhibit bands at 1750, 1742, 1722, 1709, 1703, 1683, 1669, 1659, 1652, 1645, 1636, and 1631 cm^{-1}, which are potential candidates for the νC=O vibrations. The 1750-, 1742-, and 1722-cm^{-1} bands are the only candidates for the νC_{10a}=O modes. The 1709-, 1703-, and 1683-cm^{-1} bands are the only possibilities for the νC_9=O vibrations. The remaining bands are candidates for the νC_{2a}=O modes. The X-ray crystallographic data for RC's from *Rb. sphaeroides* indicate that no hydrogen bonds exist between protein residues and the C_2-acetyl carbonyls of either BPh_L or BPh_M (Figure 1).[10c] A hydrogen bond is present between the a protein residue and the C_9-keto group of BPh_L, whereas hydrogen bonds are potentially present between residues and the C_9-keto group of BPh_M and the C_{10a}-carbomethoxy groups of both BPh's.

On the basis of the RR and crystallographic data, we assign the 1750- and 1742-cm^{-1} bands to the νC_{10a}=O modes of the free carbonyls on the two BPh's. We are not certain of the pigment affiliation of the two bands. This assignment implies that the L- and M-side tryptophans shown in Figure 1 are not strongly interacting with the C_{10}-carbomethoxy groups. An alternative assignment would associate the 1722-cm^{-1} band with a strongly interacting C_{10}-carbomethoxy group of one of the two pigments. Indeed, we previously suggested that this band was due to the νC_{10a}=O mode of BPh_L.[28a] However, on the basis of the results of the present study, we believe that a more consistent assignment of the 1722-cm^{-1} band is to a nonfundamental mode whose analogs are observed at 1726 and 1719 cm^{-1} in the cases of the accessory BCh's and P, respectively.

We assign the RR bands observed at 1709 and 1703 cm^{-1} to the νC_9=O vibrations of the free carbonyl of BPh_M and that at 1683 cm^{-1} to the hydrogen-bonded carbonyl of BPh_L. These assignments are consistent with those previously proposed on the basis of RR and FT-IR studies of RC's.[13c,17,20] These assignments indicate that the threonine residue on the M-side does not interact strongly with BPh_M despite the fact it is close enough to do so (Figure 1).[10c] It should be noted, however, that the appearance of multiple bands in the 1703–1709-cm^{-1} range (Figure 6, λ_{ex} = 363.8 nm) may be indicative of subpopulations in which there are slightly different degrees of (albeit weak) interaction with the M-side threonine.

We assign the bands at 1669 and 1659 cm^{-1} to the νC_{2a}=O vibrations of the carbonyl groups of the two BPh's. We are not certain of the pigment affiliation of the two bands. Previously, Lutz and co-workers have assigned bands near 1636 and 1631 cm^{-1} to the νC_{2a}=O modes of BPh_M and BPh_L, respectively.[17c,d,18] These frequencies imply strong hydrogen bonding to the C_2-acetyl groups of both pigments. In contrast, the X-ray crystallographic data indicate that no such interactions are possible between protein residues and either of the two BPh's (Figure 1).[10c] It is possible that water could form hydrogen bonds to the C_2-acetyl groups of the two pigments. Regardless, we believe a more consistent assignment is to attribute the 1636- and 1631-cm^{-1} RR bands to skeletal modes of BPh_M and BPh_L, respectively. This assignment brings the assignments for the BPh's into line with those of the accessory BCh's and P. The L- and M-side modes of these latter pigments are coincident and observed at 1626 and 1628 cm^{-1}, respectively. The remaining RR bands of the BPh's at 1645 and 1652 cm^{-1} are then assigned as the other skeletal fundamental and the nonfundamental vibrations, respectively. These latter bands show no clear evidence of doubling unlike the BPh modes in the 1630–1636-cm^{-1} region.

The RR spectrum of the BPh's in the 1425–1620-cm^{-1} exhibits a reasonably good correspondence with that of the accessory BCh's. There are certain differences in the frequencies of

(52) Krawczyk, S. *Biochim. Biophys. Acta* **1989**, *976*, 140–149.

analogous vibrations of the two types of pigments; however, the basic pattern of RR bands is identical. Accordingly, we have assigned the remainder of the RR spectrum of the BPh's by analogy to that of the accessory BCh's (Table II). With the exception of the band(s) in the 1580–1585-cm^{-1} region, there is no clear evidence that the frequencies of the analogous bands of BPh_L and BPh_M differ substantially. On the basis of previous RR studies of genetically modified RC's, we have assigned the double bands at 1580 and 1584 cm^{-1} to BPh_L and BPh_M, respectively.[13a,b]

C. Implications for Pigment Structure and Pigment–Protein Interactions. The vibrational assignments for the carbonyl and skeletal modes of the various pigments in the RC can be used to infer specific structural features of the BCh's and BPh's and the nature of the interactions between these pigments and the protein matrix. In the course of discussing the vibrational assignments, we noted certain features of the hydrogen-bonding interactions between the carbonyl groups and the protein matrix. In the following discussion, we focus on the structural implications of the vibrational assignments for the skeletal modes. For completeness, we briefly summarize the nature of the carbonyl–protein interactions at the beginning of the discussion for each type of pigment.

1. Accessory BCh's. The RR data for the accessory BCh's are indicative of the absence of hydrogen bonding to the C_{10}-carbomethoxy, C_9-keto, and C_2-acetyl carbonyl groups of either BCh_L or BCh_M. This result is consistent with the X-ray crystallographic data on RC's from *Rb. sphaeroides* (Figure 1).[10c] The coincidence of the RR bands due to analogous carbonyl and skeletal modes of the L- and M-side pigments implies that the structures of the macrocycles of BCh_L and BCh_M are essentially identical. The frequencies of the skeletal modes indicate that the structures of these pigments are similar to those of 5-coordinate BCh in solution.[17,24] These latter results are not consistent with the X-ray crystallographic data thus far available for RC's from *Rb. sphaeroides*. In particular, the X-ray data from the Argonne group indicate that a histidine is coordinated to both BCh_L and BCh_M and that Mg(II)–His_{L153} is 0.8 Å longer than Mg(II)–His_{M180}.[10c] In contrast, the X-ray data from the San Diego group suggest that His_{M180} is not coordinated to the Mg(II) ion of BCh_M.[9c] Either of these two different bonding situations would be expected to result in clearly observable differences in the RR frequencies of analogous modes of BCh_L versus BCh_M.[24] It should be noted, however, that the X-ray crystal structures thus far available for RC's from *Rb. sphaeroides* were determined to 2.8–3.1-Å resolution. This level of resolution may not be sufficient to determine the Mg(II)–histidine bond lengths accurately. In contrast, the X-ray crystal structure of RC's from *Rps. viridis* has been determined to 2.3 Å.[8] This structure indicates that the Mg(II)–histidine bond lengths of the two BCh's differ by at most 0.1 Å. A bond length difference of this magnitude would not be expected to result in dramatically different frequencies for the skeletal modes of the two different accessory BCh's. Accordingly, the RR data we present here for RC's from *Rb. sphaeroides* are more consistent with the structural data reported for *Rps. viridis*.

2. Special Pair BCh's. The vibrational data for P indicate the absence of hydrogen bonding to the C_{10}-carbomethoxy, C_9-keto, and C_2-acetyl carbonyl groups of P_M and the C_9-keto group of P_L; hydrogen bonding occurs to the C_{10}-carbomethoxy and C_2-acetyl carbonyl groups of P_L. These results are consistent with the X-ray crystallographic data for *Rb. sphaeroides* (Figure 1).[10c] The lack of coincidence of certain RR bands of P_L and P_M suggests that the structures of the macrocycles of the two pigments are not identical. The fact that the skeletal mode frequencies of one pigment of P are similar to those of the accessory BCh's implies that the structure of this macrocycle is similar to that of the BCh's (and to 5-coordinate BCh in solution[17,24]). The lower skeletal mode frequencies observed for the other pigment could arise from any one of several types of structural perturbations. An unusually long Mg(II)–histidine bond length would allow the metal ion to relax into the plane of the ring. This would result in an expanded macrocycle core and consequently lower the skeletal mode frequencies.[23–25,53] Alternatively, an unusually short Mg(II)–histidine bond length would pull the metal ion further out of plane. This would result in a more conformationally distorted macrocycle which would also have lower skeletal mode frequencies.[53f,54]

As was previously noted, the X-ray crystallographic data for RC's provide no definitive insights as to the nature of the structural perturbations that might be responsible for the differences in the frequencies of the skeletal modes of P_L versus P_M. In particular, both sets of crystallographic data obtained for *Rb. sphaeroides* indicate that Mg(II)–His_{L173} is longer than Mg(II)–His_{M200}.[9c,10c] This would nominally suggest that the core size of P_L would be larger than that of P_M, thus giving rise to a lower set of skeletal mode frequencies. The Argonne structure indicates that the Mg(II)–His_{M200} bond length is ~2.2 Å,[10c] which is similar to the Mg(II)–histidine bond lengths of the accessory BCh's in RC's from *Rps. viridis*.[8] The San Diego structure suggests that the Mg(II)–His_{M200} bond length is less than ~3.0 Å.[9c] Both structures indicate that the Mg(II)–His_{L173} bond length is unusually long (~3.2 and 4.0 Å, respectively). Although the RR data are in qualitative agreement with the Argonne structure, which indicates that one pigment (P_L) has a normal Mg(II)–histidine bond length, they are not consistent with the large bond-length differences (1.0 Å) predicted for P_L versus P_M. Such large bond-length differences would be expected to lead to a significant disparity in the core sizes. This, in turn, would result in much larger frequency differences (as much as 20 cm^{-1})[23–25,53] for analogous skeletal modes than are observed in this study (~6 cm^{-1}, Table II). In general, core size differences would also be expected to result in different frequencies for all of the skeletal modes of the ring. However, only RR bands in the 1480–1530-cm^{-1} region appear to be doubled. It is possible that the bands of other skeletal modes are also doubled but the splittings are lost in spectral congestion. However, this is not a particularly satisfying explanation.

The X-ray crystallographic data for RC's from *Rps. viridis* provide some additional insight into the structural differences between P_L and P_M.[8] Unlike the X-ray data reported for *Rb. sphaeroides*,[9c,10c] these data indicate that the two Mg(II)–histidine bond lengths in P are near normal and differ only slightly [Mg(II)–His_{L173} ~2.2 Å; Mg(II)–His_{M200} ~1.9 Å]. This relatively small bond-length difference would be expected to give rise to relatively small frequency differences for analogous skeletal modes of P_L and P_M. Accordingly, the X-ray crystallographic data reported for *Rps. viridis* is qualitatively in better agreement with the RR data for *Rb. sphaeroides* than is the structural data for the latter protein. It should also be noted that the X-ray data for *Rps. viridis* indicate that the Mg(II)–His_{M200} bond length is similar to that of the Mg(II)–histidine bond lengths of the accessory BCh's whereas the Mg(II)–His_{L173} bond length is

(53) (a) Spaulding, L. D.; Chang, C. C.; Yu, N.-T.; Felton, R. H. *J. Am. Chem. Soc.* **1975**, 97, 2517–2525. (b) Choi, S.; Spiro, T. G.; Langry, K. C.; Smith, K. M.; Budd, D. L.; Lamar, G. N. *J. Am. Chem. Soc.* **1982**, *104*, 4345–4351. (c) Spiro, T. G. In *Iron Porphyrins*; Lever, A. P. B., Gray, H. B., Eds.; Addison-Wesley: Reading, MA, 1983; Vol. 2, pp 89–159. (d) Oertling, W. A.; Salehi, A.; Chung, Y. C.; Leroi, G. E.; Chang, C. K.; Babcock, G. T. *J. Phys. Chem.* **1987**, *91*, 5887–5898. (e) Parthasarati, N.; Hansen, C.; Yamaguchi, S.; Spiro, T. G. *J. Am. Chem. Soc.* **1987**, *109*, 3865–3871. (f) Prendergast, K.; Spiro, T. G. *J. Am. Chem. Soc.* **1992**, *114*, 3793–3801.

(54) (a) Shelnutt, J. A.; Alson, K.; Ho, J.-H.; Yu, N.-T.; Yamamoto, T.; Rifkind, J. M. *Biochemistry* **1986**, *25*, 620–627. (b) Brennan, T. D.; Scheidt, W. R.; Shelnutt, J. A. *J. Am. Chem. Soc.* **1988**, *110*, 3919–3924. (c) Alden, R. G.; Crawford, B. A.; Doolen, R.; Ondrias, M. R.; Shelnutt, J. A. *J. Am. Chem. Soc.* **1989**, *111*, 2070–2072. (d) Barkigia, K. M.; Berber, M. D.; Fajer, J.; Medforth, C. J.; Renner, M. W.; Smith, K. M. *J. Am. Chem. Soc.* **1990**, *112*, 8851–8857. (e) Alden, R. G.; Ondrias, M. R.; Shelnutt, J. A. *J. Am. Chem. Soc.* **1990**, *112*, 691–697. (f) Shelnutt, J. A.; Medforth, C. J.; Berber, M. D.; Barkigia, K. M.; Smith, K. M. *J. Am. Chem. Soc.* **1991**, *113*, 4077–4087. (g) Sparks, L. D.; Medforth, C. J.; Park, M.-S.; Chamberlain, J. R.; Ondrias, M. R.; Senge, M. O.; Smith, K. M.; Shelnutt, J. A. *J. Am. Chem. Soc.* **1993**, *115*, 581–592. (h) Stichternath, A.; Schweitzer-Stenner, R.; Dreybrodt, W.; Mak, R. S. W.; Li, X.-Y.; Sparks, L. D.; Shelnutt, J. A.; Medforth, C. J.; Smith, K. M. *J. Phys. Chem.* **1993**, *97*, 3701–3708.

shorter.[8] The crystallographic data also indicate that the macrocycle of P_M is more distorted from planarity than that of P_L. Collectively, these data suggest that the lower set of skeletal mode frequencies should be associated with P_M. An unusual conformational distortion might also explain the observation that only certain skeletal modes exhibit different frequencies in P_L versus P_M. Regardless, a clearer picture of the structural differences between these two pigments must await further refinements in the X-ray structure of RC's from *Rb. sphaeroides*.

3. BPh's. The RR data for the BPh's are indicative of the absence of significant hydrogen bonding to the C_{10}-carbomethoxy, C_9-keto, and C_2-acetyl groups of BPh_M as well as the C_{10}-carbomethoxy and C_2-acetyl groups of BPh_L. The vibrational data are also consistent with strong hydrogen bonding to the C_9=O group of BPh_L. The absence of hydrogen bonds to the C_{10}-carbomethoxy groups of both pigments and the weak hydrogen bond to the C_9-keto group of BPh_M indicates that pigment–protein interactions inferred from X-ray crystallographic data for RC's from *Rb. sphaeroides* (Figure 1)[10c] are in fact absent. The coincidence of the RR bands of most of the analogous skeletal modes of BPh_L and BPh_M indicates that structures of the macrocycles of these two pigments are very similar. The frequencies of the skeletal modes further suggest that the structures of the pigments in the RC are for the most part similar to those of BPh in solution.[17] Only two skeletal vibrations exhibit different frequencies for BPh_L versus BPh_M. These two modes are primarily comprised of internal coordinates on rings III and V (Table II, Figure 11). Accordingly, the RR data suggest that the two pigments differ in structure only in this region of the macrocycle. The structural differences between BPh_L and BPh_M are attributed to the presence of the strong interaction between the C_9-keto group of BPh_L and the Glu_{L104} protein residue. An equivalent interaction is absent in the M-subunit (vide supra). In particular, RR studies of genetically modified RC's where the hydrogen-bonding Glu_{L104} residue is changed to a non-hydrogen-bonding leucine have shown that the frequency difference observed for the $\sim$1580-cm^{-1} RR bands of the two BPh's in the wild-type RC is absent in the mutant.[13a,b] Accordingly, the removal of the interaction between BPh_L and the protein appears to remove the structural difference between the two BPh's.

V. Summary and Conclusions

RR spectra have been obtained for RC's from *Rb. sphaeroides* by using a large number of excitation wavelengths which span the B_x, B_y, Q_x, and Q_y absorption bands of the different bacteriochlorin pigments in the protein. The number of exciting lines and their wavelengths allow reasonably selective excitation of the different pigments and permit the observation of the full complement of RR bands from the individual pigments. A comprehensive set of vibrational assignments has been obtained for the high-frequency carbonyl and skeletal modes of the six different bacteriochlorin cofactors in the RC. These assignments serve as benchmarks for interpreting the spectra of genetically modified RC's[13,15] and for evaluating spectral changes observed in time-resolved vibrational experiments.[20e,f,32] The RR studies show that any conclusions regarding the structures of the pigments or their interaction with the protein matrix must involve the analysis of a large number of vibrational modes rather than a select few. Accordingly, structural characteristics predicted on the basis of previous vibrational studies (both static and time-resolved) of RC's must be reconsidered in light of the complete set of assignments. The data reported herein indicate that the structures of the two accessory BCh's are similar to one another and similar to that of BCh in solution. The structures of the two BPh's are also quite similar and similar to that of BPh in solution. In contrast, the structures of the two BCh's in P appear to be different. The vibrational data indicate that one pigment is structurally similar to the accessory BCh's whereas the other either has an expanded macrocycle core or is more conformationally distorted. The exact origin of these structural differences between P_L and P_M is not clear. It also remains to be determined whether these structural differences have any effect on the functional characteristics of the protein, such as the path specificity and detailed kinetics of electron transfer.[11,12j,k,14f,55-59]

Acknowledgment. This work was support by Grants GM36243 (D.F.B.) and GM30353 (H.A.F.) from the National Institute of General Medical Sciences and the Cooperative State Research Service, USDA, under agreement no.92-37306-7690 (H.A.F.).

(55) (a) Holzafel, W.; Finkele, U.; Kaiser, W.; Oesterhelt, D.; Scheer, H.; Stiltz, H. U.; Zinth, W. *Chem. Phys. Lett.* **1989**, *161*, 1–7. (b) Holzafel, W.; Finkele, U.; Kaiser, W.; Oesterhelt, D.; Scheer, H.; Stiltz, H. U.; Zinth, W. *Proc. Natl. Acad. Sci. U.S.A.* **1990**, *87*, 5168–5172. (c) Lauterwasser, C.; Finkele, U.; Scheer, H.; Zinth, W. *Chem. Phys. Lett.* **1991**, *183*, 471–477.

(56) Holten, D.; Kirmaier, C. *Proc. Natl. Acad. Sci. U.S.A.* **1990**, *87*, 3552–3556.

(57) (a) Vos, M. H.; Lambry, J.-C.; Robles, S. J.; Youvan, D. C.; Breton, J.; Martin, J.-L. *Proc. Natl. Acad. Sci. U.S.A.* **1991**, *88*, 8885–8889. (b) Vos, M. H.; Lambry, J.-C.; Robles, S. J.; Youvan, D. C.; Breton, J.; Martin, J.-L. *Proc. Natl. Acad. Sci. U.S.A.* **1992**, *89*, 8885–8889.

(58) Chan, C.-K.; DiMagno, T. J.; Chen, L. X.-Q.; Norris, J. R.; Fleming, G. R. *Proc. Natl. Acad. Sci. U.S.A.* **1991**, *88*, 11202–11207.

(59) Small, G. J.; Hayes, J. M.; Silbey, R. J. *J. Phys. Chem.* **1991**, *96*, 7499–7501.